

CP Violation 2HDM from collider to EDM

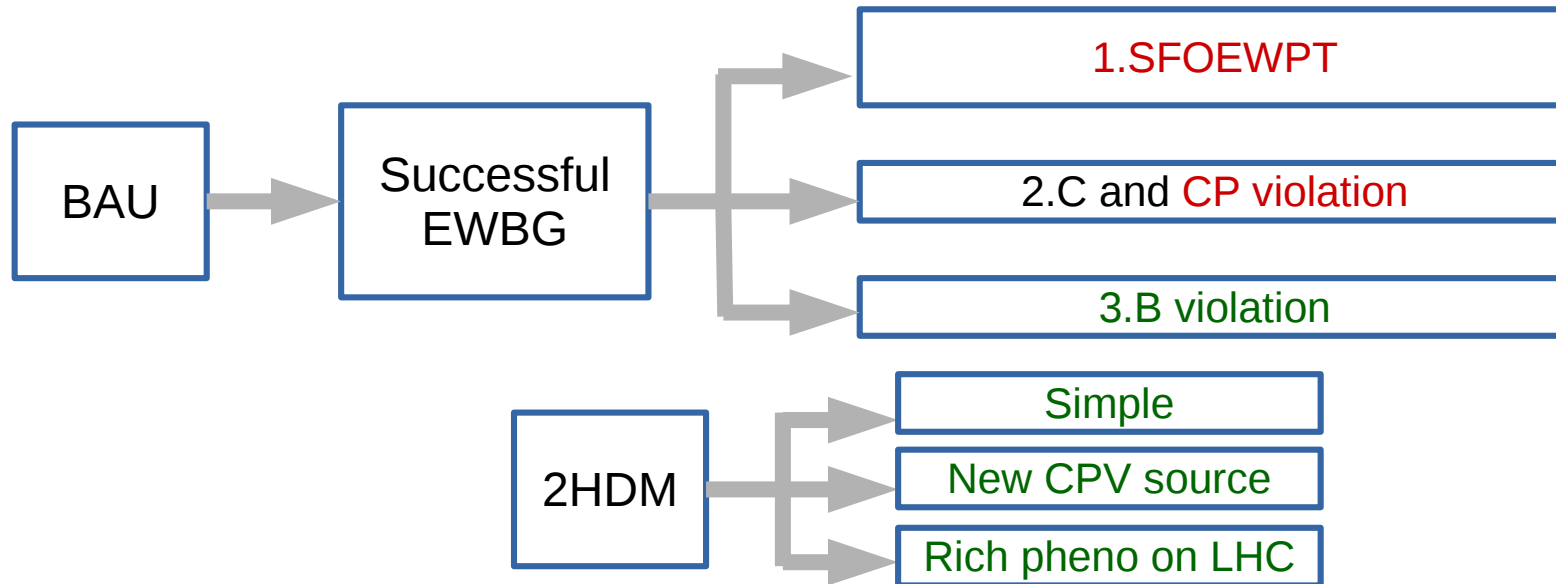
Hao-Lin Li

Amherst Center for Fundamental Interaction (ACFI)
University of Massachusetts Amherst

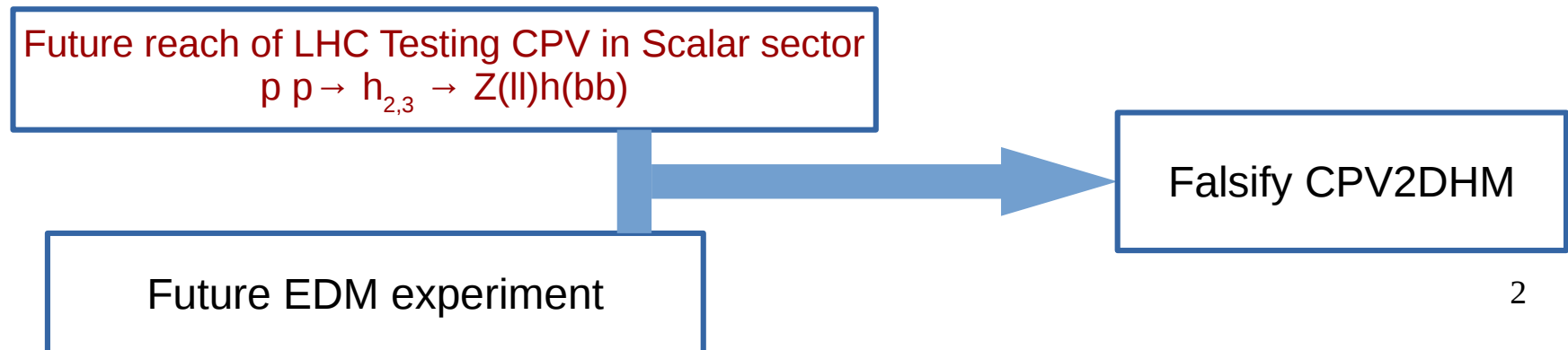
C.-Y. Chen, H.-L. Li, M.J. Ramsey-Musolf, Phys.Rev. D97 (2018) no.1, 015020

Motivation and Goal

- Motivation



- Goal:



Outline

- Introduction of CPV 2HDM
- Collider Phenomenology
- EDM limit
- Results
- Summary

General 2HDM

- Lagrangian:

$$\begin{aligned} V(\phi_1, \phi_2) = & -\frac{1}{2} \left[m_{11}^2 (\phi_1^\dagger \phi_1) + \left(m_{12}^2 (\phi_1^\dagger \phi_2) + \text{h.c.} \right) + m_{22}^2 (\phi_2^\dagger \phi_2) \right] \\ & + \frac{\lambda_1}{2} (\phi_1^\dagger \phi_1)^2 + \frac{\lambda_2}{2} (\phi_2^\dagger \phi_2)^2 + \lambda_3 (\phi_1^\dagger \phi_1) (\phi_2^\dagger \phi_2) + \lambda_4 (\phi_1^\dagger \phi_2) (\phi_2^\dagger \phi_1) \\ & + \frac{1}{2} \left[\lambda_5 (\phi_1^\dagger \phi_2)^2 + \lambda_6 (\phi_1^\dagger \phi_2) (\phi_1^\dagger \phi_1) + \lambda_7 (\phi_1^\dagger \phi_2) (\phi_2^\dagger \phi_2) + \text{h.c.} \right] . \end{aligned}$$

4 parameters can be complex and potential to trigger CP violation:

$$m_{12}^2 \quad \lambda_5 \quad \lambda_6 \quad \lambda_7$$

2HDM with Z_2

- Z_2 symmetry: Preventing Tree level FCNC

$$Z_2 \quad : \quad \phi_1 \rightarrow -\phi_1 \quad \phi_2 \rightarrow \phi_2$$

$$Q_L \rightarrow Q_L \quad L \rightarrow L$$

No CPV if exact, so soft break retain non-zero m_{12}^2

Model	u_R	d_R	e_R
Type-I	+	+	+
Type-II	+	-	-
Lepton-Specific	+	+	-
Flipped	+	-	+

Only two parameter can be complex:

$$m_{12}^2 \quad \lambda_5 \quad \lambda_6 = \lambda_7 = 0$$

2HDM with Z_2

- After EWSB

$$\langle \phi_1 \rangle = \begin{pmatrix} 0 \\ v_1 e^{i\delta_1} \end{pmatrix} \quad \langle \phi_2 \rangle = \begin{pmatrix} 0 \\ v_2 e^{i\delta_2} \end{pmatrix} \quad \tan \beta = v_2/v_1$$

- Subset of $U(2)$ that keeps $\lambda_6 = \lambda_7 = 0$

$$e^{i\psi} \begin{pmatrix} 1 & 0 \\ 0 & e^{i\chi} \end{pmatrix} \quad e^{i\psi} \begin{pmatrix} 0 & 1 \\ e^{i\chi} & 0 \end{pmatrix}$$

absorb the phase in the vev without loose generality

m_{12}^2 and λ_5 are **not Independent** related by the minimization condition of potential:

$$\text{Im}(m_{12}^2) = v_1 v_2 \text{Im}(\lambda_5) \quad \Rightarrow \quad \text{Only one phase related parameter}$$

α_b

2HDM with Z_2

- Changing parameter set
In the unitary gauge:

$$\phi_1 = \begin{pmatrix} -\sin \beta H^+ \\ \frac{1}{\sqrt{2}}(v \cos \beta + H_1^0 - i \sin \beta A^0) \end{pmatrix}, \quad \phi_2 = \begin{pmatrix} \cos \beta H^+ \\ \frac{1}{\sqrt{2}}(v \sin \beta + H_2^0 + i \cos \beta A^0) \end{pmatrix}$$

$$\lambda_1, \lambda_2, \lambda_3, \lambda_4, \text{Im} \lambda_5, \text{Re} \lambda_5, \text{Re} m_{12}^2, \text{Im} m_{12}^2, m_{11}^2, m_{22}^2$$

Minimization
condition (3)



Mass of charge Higgs (1)

Diagonalization of neutral Mass matrix (6)

$$v, \tan \beta, \nu, \alpha, \alpha_b, \alpha_c, m_{h_1}, m_{h_2}, m_{h_3}, m_{h_H^+}$$

$$\nu = \frac{\text{Re} m_{12}^2}{v^2 \sin 2\beta}$$

2HDM with Z_2

- Changing parameter set
In the unitary gauge:

$$\phi_1 = \begin{pmatrix} -\sin \beta H^+ \\ \frac{1}{\sqrt{2}}(v \cos \beta + H_1^0 - i \sin \beta A^0) \end{pmatrix}, \quad \phi_2 = \begin{pmatrix} \cos \beta H^+ \\ \frac{1}{\sqrt{2}}(v \sin \beta + H_2^0 + i \cos \beta A^0) \end{pmatrix}$$

$$\lambda_1, \lambda_2, \lambda_3, \lambda_4, \text{Im} \lambda_5, \text{Re} \lambda_5, \text{Re} m_{12}^2, \text{Im} m_{12}^2, m_{11}^2, m_{22}^2$$

Minimization
condition (3)

Mass of charge Higgs (1)

Diagonalization of neutral Mass matrix (6)

$$v, \tan \beta, \nu, \alpha, \alpha_b, \alpha_c, m_{h_1}, m_{h_2}, m_{h_3}, m_{h_H^+}$$

$$\nu = \frac{\text{Re} m_{12}^2}{v^2 \sin 2\beta}$$

2HDM with Z_2

- Changing parameter set
In the unitary gauge:

$$\phi_1 = \begin{pmatrix} -\sin \beta H^+ \\ \frac{1}{\sqrt{2}}(v \cos \beta + H_1^0 - i \sin \beta A^0) \end{pmatrix}, \quad \phi_2 = \begin{pmatrix} \cos \beta H^+ \\ \frac{1}{\sqrt{2}}(v \sin \beta + H_2^0 + i \cos \beta A^0) \end{pmatrix}$$

$$\lambda_1, \lambda_2, \lambda_3, \lambda_4, \text{Im} \lambda_5, \text{Re} \lambda_5, \text{Re} m_{12}^2, \text{Im} m_{12}^2, m_{11}^2, m_{22}^2$$

Minimization
condition (3)

Mass of charge Higgs (1)

Diagonalization of neutral Mass matrix (6)

$$v, \tan \beta, \nu, \alpha, \alpha_b, \alpha_c, m_{h_1}, m_{h_2}, m_{h_3}, m_{h_H^+}$$

$$\nu = \frac{\text{Re} m_{12}^2}{v^2 \sin 2\beta}$$

2HDM with Z_2

- Diagonalization of neutral Higgs mass matrix

$$RM_n^2 R^T = \text{diag}(m_{h_1}^2, m_{h_2}^2, m_{h_3}^2) \quad (h_1, h_2, h_3) = (H_1^0, H_2^0, A^0)R$$

$$R = R_{23}(\alpha_c)R_{13}(\alpha_b)R_{12}(\alpha + \pi/2)$$

$$-\frac{\pi}{2} < \alpha_c, \alpha_b, \alpha \leq \frac{\pi}{2}$$

$$M_n^2 = v^2 \begin{pmatrix} \lambda_1 c_\beta^2 + \nu s_\beta^2 & (\lambda_{345} - \nu)c_\beta s_\beta & -\frac{1}{2} \text{Im } \lambda_5 s_\beta \\ (\lambda_{345} - \nu)c_\beta s_\beta & \lambda_2 s_\beta^2 + \nu c_\beta^2 & -\frac{1}{2} \text{Im } \lambda_5 c_\beta \\ -\frac{1}{2} \text{Im } \lambda_5 s_\beta & -\frac{1}{2} \text{Im } \lambda_5 c_\beta & -\text{Re } \lambda_5 + \nu \end{pmatrix}$$

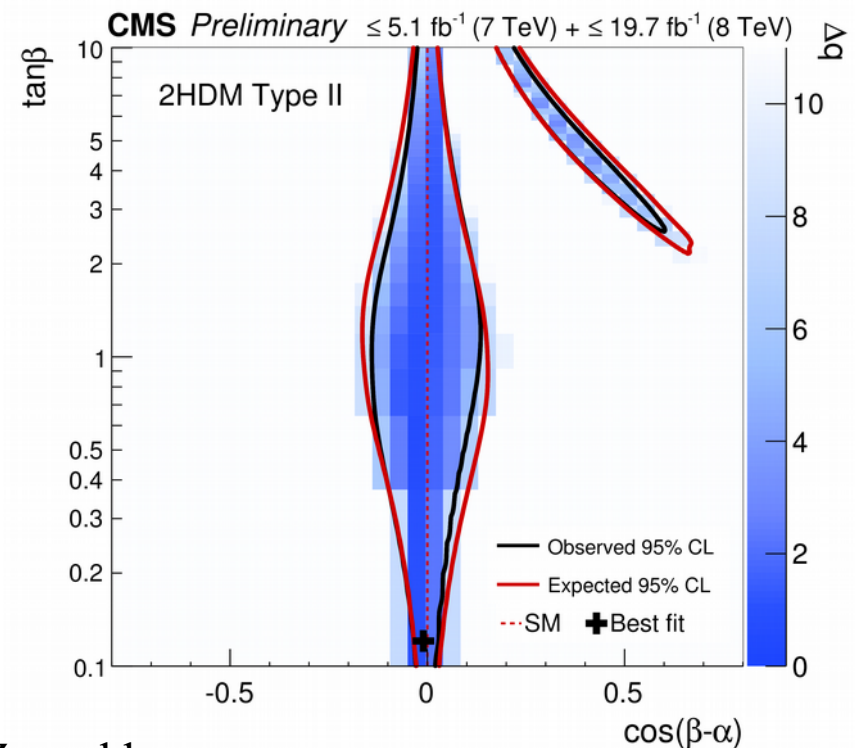
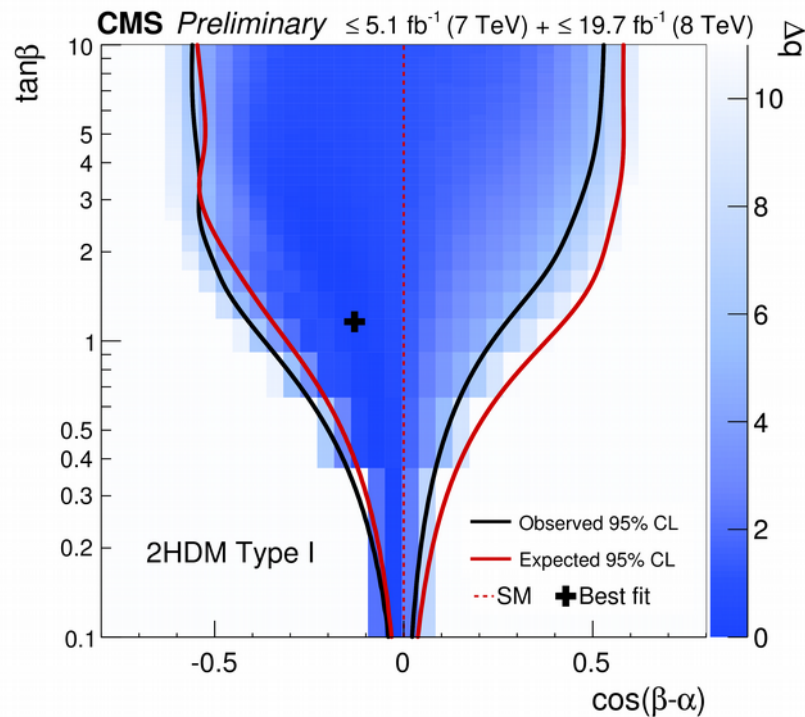
Non-vanishing $\text{Im } \lambda_5$ signals the mixing between CP even and CP odd Higgs, i.e. trigger CP Violation in the scalar sector.

$$\alpha_c = \begin{cases} \alpha_c^-, & \alpha + \beta \leq 0 \\ \alpha_c^+, & \alpha + \beta > 0 \end{cases}, \quad \tan \alpha_c^\pm = \frac{\mp |\sin \alpha_b^{\max}| \pm \sqrt{\sin^2 \alpha_b^{\max} - \sin^2 \alpha_b}}{\sin \alpha_b} \sqrt{\frac{m_{h_3}^2 - m_{h_1}^2}{m_{h_2}^2 - m_{h_1}^2}}.$$

Collider Phenomenology

Collider Phenomenology

- SM-like Higgs global fit favor alignment limit:



CMS Collaboration, Report No. CMS-PAS-HIG-16-007.

$$\cos(\beta - \alpha) \sim 0$$

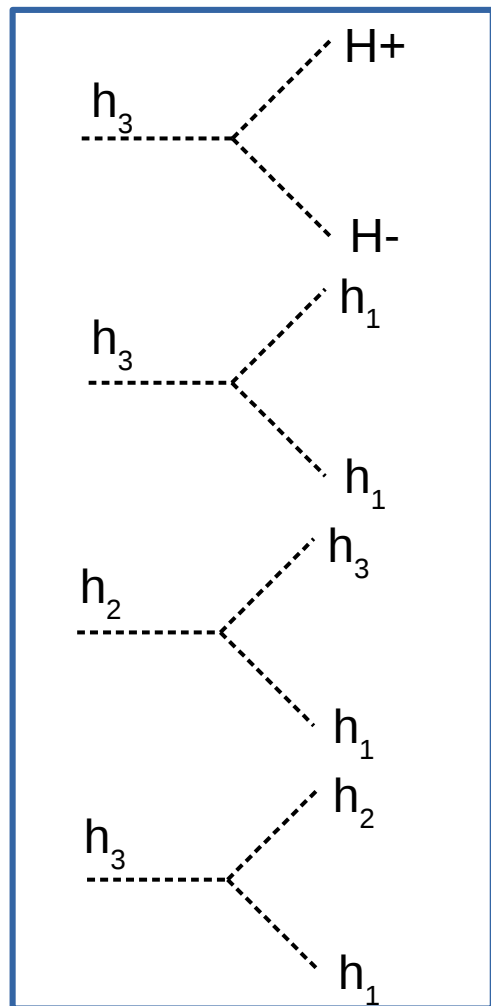
$$h_1 \rightarrow WW, ZZ, \gamma\gamma, bb, \tau\tau$$

Parametrize the deviation by:

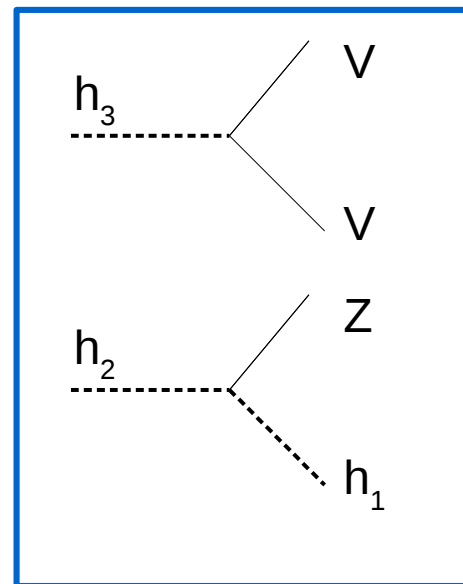
$$\beta - \alpha = \pi/2 + \theta$$

Collider Phenomenology

- Possible new channel sensitive to CP violation



Hard to use on-shell enhancement, by pheno constraints or interference with other process



Potential to use on-shell enhancement.

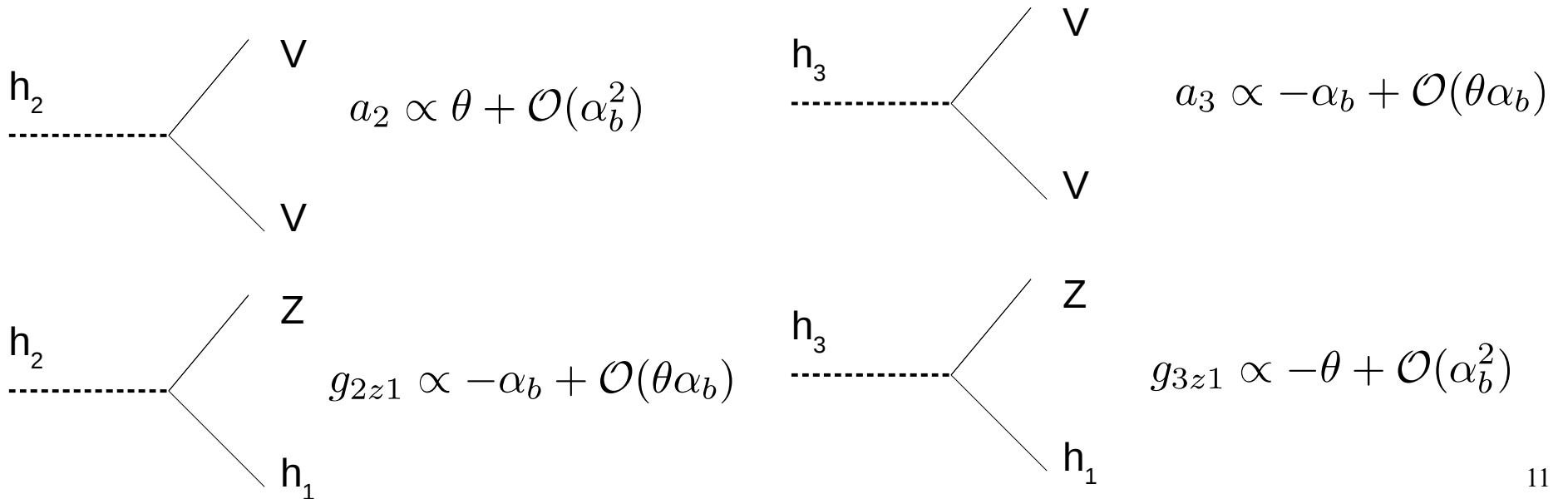
R. Gröber, M. Mühlleitner, M. Spira, Nucl.Phys. B925 (2017) 1-27
 A. G. Akeroyd et al., Eur. Phys. J. C 77, 276 (2017)
 C. Y. Chen, S. Dawson and Y. Zhang, JHEP 1506, 056 (2015)

2HDM with Z_2

- Higgs couplings:

$$\begin{aligned}\mathcal{L}_{int} &= -\frac{m_f}{v}h_i (c_{f,i}\bar{f}f + \tilde{c}_{f,i}\bar{f}i\gamma_5 f) \\ &+ a_i h_i \left(\frac{2m_W^2}{v}W_\mu W^\mu + \frac{m_Z^2}{v}Z_\mu Z^\mu \right) \\ &+ g_{iz1}Z^\mu((\partial_\mu h_i)h_1 - h_i\partial_\mu h_1)\end{aligned}$$

Two types of new couplings:

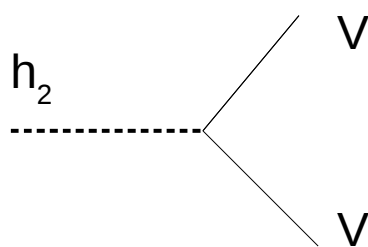


2HDM with Z_2

- Higgs couplings:

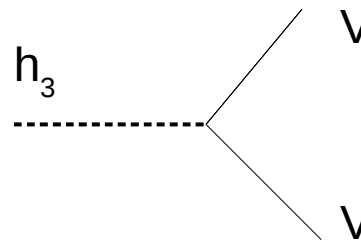
$$\begin{aligned}\mathcal{L}_{int} = & -\frac{m_f}{v}h_i(c_{f,i}\bar{f}f + \tilde{c}_{f,i}\bar{f}i\gamma_5 f) \\ & + a_i h_i \left(\frac{2m_W^2}{v}W_\mu W^\mu + \frac{m_Z^2}{v}Z_\mu Z^\mu \right) \\ & + g_{iz1}Z^\mu((\partial_\mu h_i)h_1 - h_i\partial_\mu h_1)\end{aligned}$$

Two types of new couplings:



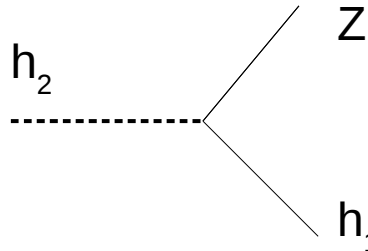
h_2 (dashed line) splits into two V (solid lines).

$a_2 \propto \theta + \mathcal{O}(\alpha_b^2)$



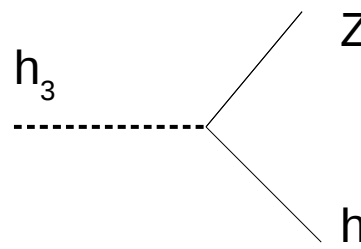
h_3 (dashed line) splits into two V (solid lines).

$a_3 \propto -\alpha_b + \mathcal{O}(\theta\alpha_b)$



h_2 (dashed line) splits into Z (solid line) and h_1 (solid line).

$g_{2z1} \propto -\alpha_b + \mathcal{O}(\theta\alpha_b)$

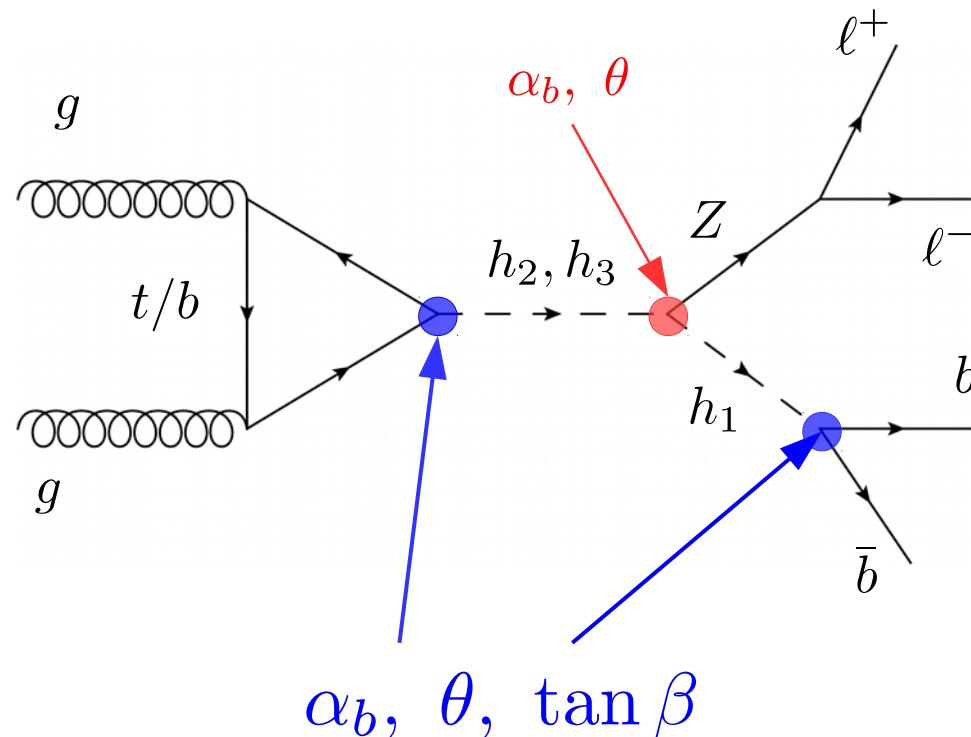


h_3 (dashed line) splits into Z (solid line) and h_1 (solid line).

$g_{3z1} \propto -\theta + \mathcal{O}(\alpha_b^2)$

Collider Phenomenology

- In the following we will focus on the process




Derive the prospective upper limit on
 $\sigma(pp \rightarrow h_{2,3})\text{Br}(h_{2,3} \rightarrow Zh_1)\text{Br}(h_1 \rightarrow b\bar{b})$
 in future 14TeV LHC and project this limit onto the
 $|\sin\alpha_b|$ vs $\tan\beta$



Collider Phenomenology

- ATLAS 8TeV analysis revisit ($p p \rightarrow A \rightarrow Z(l l) h(b b)$)
- 2e or 2 opposite sign μ , with $P_t > 7$ GeV and $|\eta_e|(|\eta_\mu|) < 2.5(2.7)$,
- Exactly 2 b tagged jets, with $P_{T,b}^{\text{lead}} > 45$ GeV and $P_{T,b}^{\text{sub}} > 20$ GeV,
- $83 < m_{ll} < 95$, and $95 < m_{bb} < 135$.
- $E_T^{\text{miss}}/\sqrt{H_T} < 3.5$ GeV^{1/2}
- $P_T^Z > 0.44 M_{h2,3} - 106$ GeV




Collider Phenomenology

- ATLAS 8TeV analysis revisit
- 2e or 2 opposite sign μ , with $P_t > 7$ GeV and $|\eta_e|(|\eta_\mu|) < 2.5(2.7)$,
- Exactly 2 b tagged jets, with $P_{T,b}^{\text{lead}} > 45$ GeV and $P_{T,b}^{\text{sub}} > 20$ GeV,
- $83 < m_{ll} < 95$, and $95 < m_{bb} < 135$.  Reduce diboson background
- $E_T^{\text{miss}}/\sqrt{H_T} < 3.5$ GeV^{1/2}
- $P_T^Z > 0.44 M_{h2,3} - 106$ GeV

Collider Phenomenology

- ATLAS 8TeV analysis revisit
- 2e or 2 opposite sign μ , with $P_t > 7$ GeV and $|\eta_e|(|\eta_\mu|) < 2.5(2.7)$,
- Exactly 2 b tagged jets, with $P_{T,b}^{\text{lead}} > 45$ GeV and $P_{T,b}^{\text{sub}} > 20$ GeV,
- $83 < m_{ll} < 95$, and $95 < m_{bb} < 135$.  Reduce diboson background
- $E_T^{\text{miss}}/\sqrt{H_T} < 3.5$ GeV^{1/2}  Reduce ttbar background
- $P_T^Z > 0.44 M_{h2,3} - 106$ GeV

Collider Phenomenology

- ATLAS 8TeV analysis revisit
- 2e or 2 opposite sign μ , with $P_t > 7$ GeV and $|\eta_e|(|\eta_\mu|) < 2.5(2.7)$,
- Exactly 2 b tagged jets, with $P_{T,b}^{\text{lead}} > 45$ GeV and $P_{T,b}^{\text{sub}} > 20$ GeV,
- $83 < m_{ll} < 95$, and $95 < m_{bb} < 135$.  Reduce diboson background
- $E_T^{\text{miss}}/\sqrt{H_T} < 3.5 \text{ GeV}^{1/2}$  Reduce ttbar background
- $P_T^Z > 0.44 M_{h2,3} - 106 \text{ GeV}$  Reduce Zbb and SM Zh background

Collider Phenomenology

- Comparasion between ATLAS result and ours

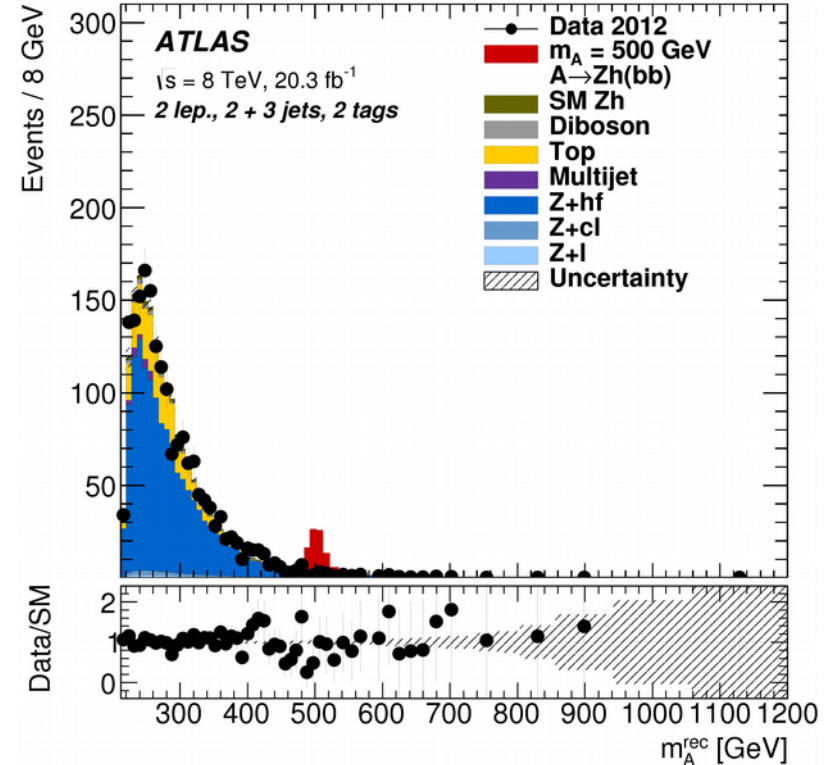
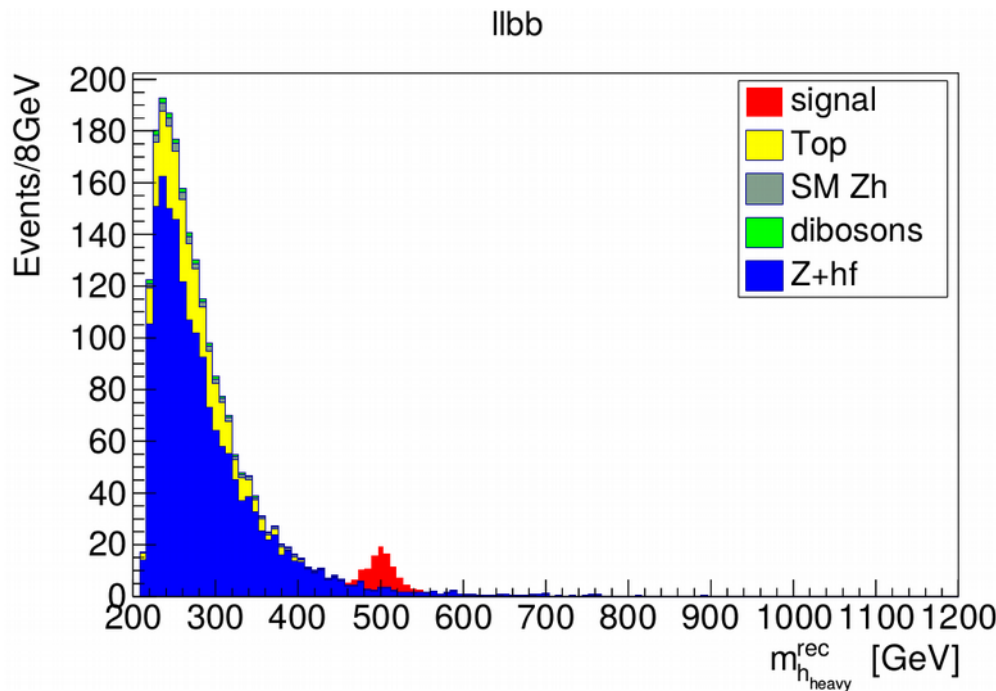
Madgraph, Pythia, Delphes

Backgrounds/ Signal	$\sigma(\text{pb})$	$\sigma \times \int \mathcal{L}$	simulated # of events after cuts	# of expected event in Ref. 30	$A \times \epsilon$
$Z(\ell\ell)bb$	12.91	2.620×10^5	1,788	1443 ± 60	6.825×10^{-3}
$t(bl\nu)\bar{t}(bl\nu)$	18.12	3.678×10^5	359	317 ± 28	9.761×10^{-4}
SM $Z(\ell\ell)h(bb)$	0.02742	5.566×10^2	47	31 ± 1.8	8.443×10^{-2}
Diboson($Z(\ell\ell)Z(bb)$)	0.2122	4.308×10^3	28	30 ± 5	6.679×10^{-3}

Two major Backgrounds

Collider Phenomenology

- Comparasion between ATLAS result and ours

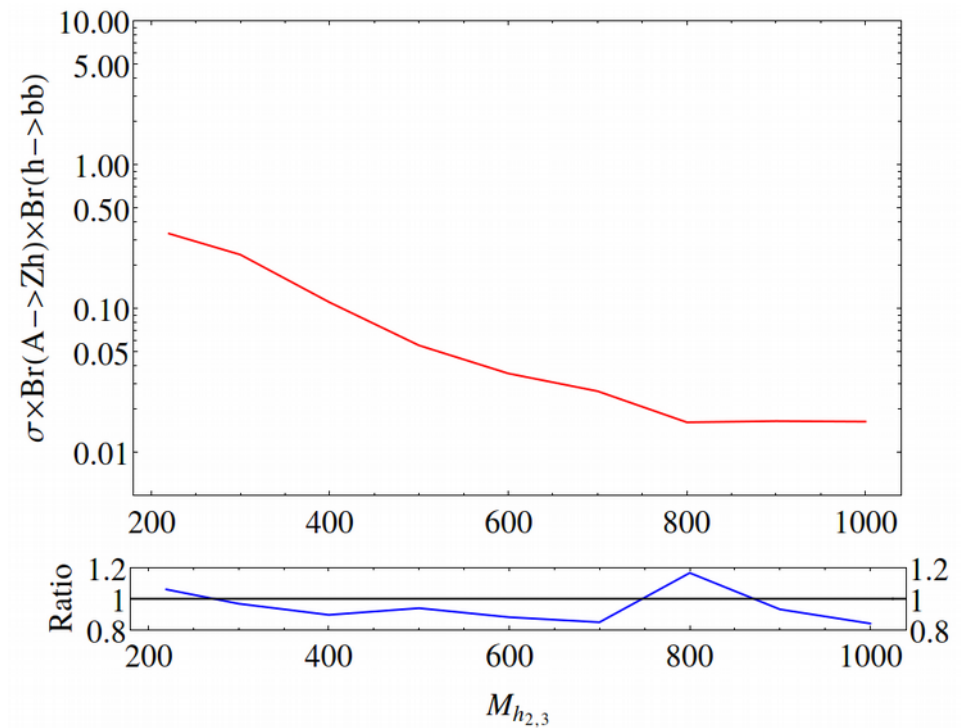
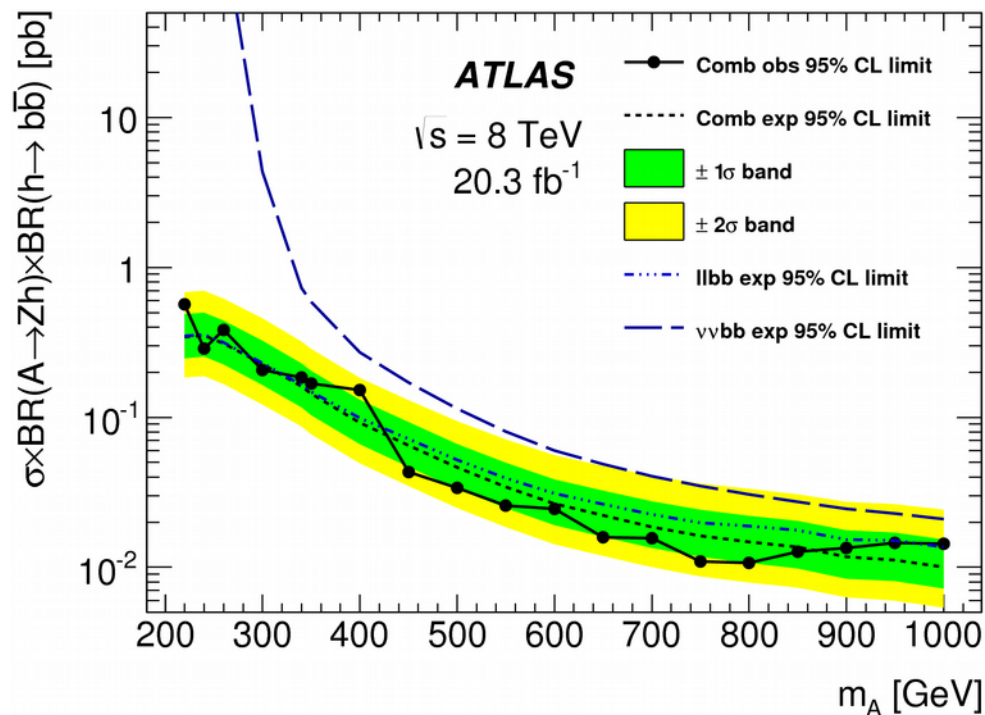


ATLAS Collaboration Phys.Lett. B744 (2015) 163-183

C.-Y. Chen, H.-L. Li, M.J. Ramsey-Musolf, Phys.Rev. D97 (2018) no.1, 015020

Collider Phenomenology

- ATLAS 8TeV analysis revisit



We reproduce the ATLAS results very well.

Collider Phenomenology

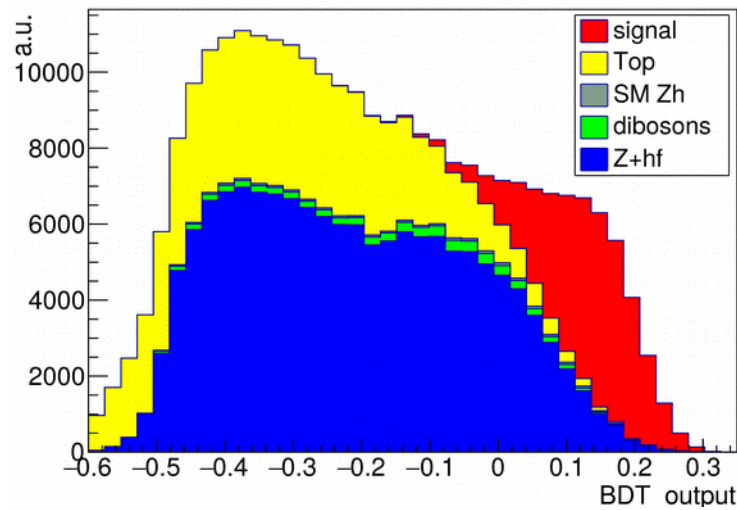
- 14 TeV forecast
- First select two leptons and two b tagged jets with same kinematic cuts:
- 2e or 2 opposite sign μ , with $P_t > 7$ GeV and $|\eta_e|(|\eta_\mu|) < 2.5(2.7)$,
- Exactly 2 b tagged jets, with $P_{T,b}^{\text{lead}} > 45$ GeV and $P_{T,b}^{\text{sub}} > 20$ GeV,
- Then we compute following quantities as inputs for Boosted Decision Tree(BDT) to optimize the selection.

$$p_{T,\ell}^{\text{lead}}, p_{T,\ell}^{\text{sub}}, p_{T,b}^{\text{lead}}, p_{T,b}^{\text{sub}}, m_{\ell\ell}, m_{bb}, p_T^Z, p_T^h, E_T^{\text{miss}} / \sqrt{H_T}, \Delta R_{\ell\ell}, \Delta R_{jj}, \Delta R_{Zh}, \Delta\phi_{Zh},$$

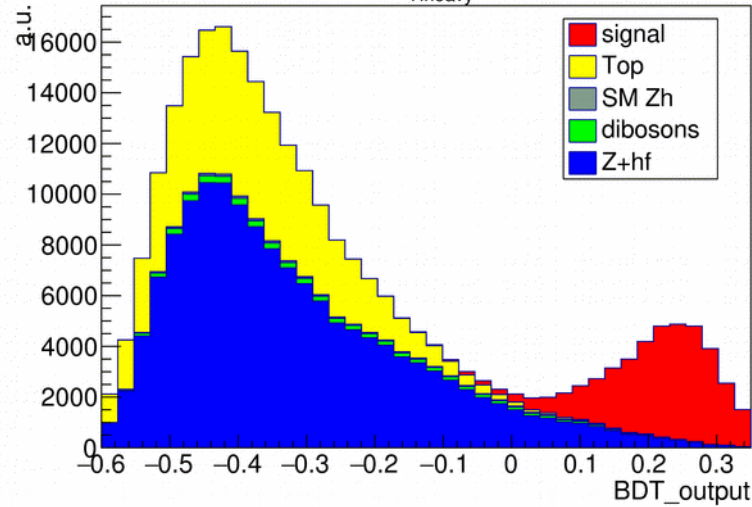
Collider Phenomenology

- Distribution for BDT score

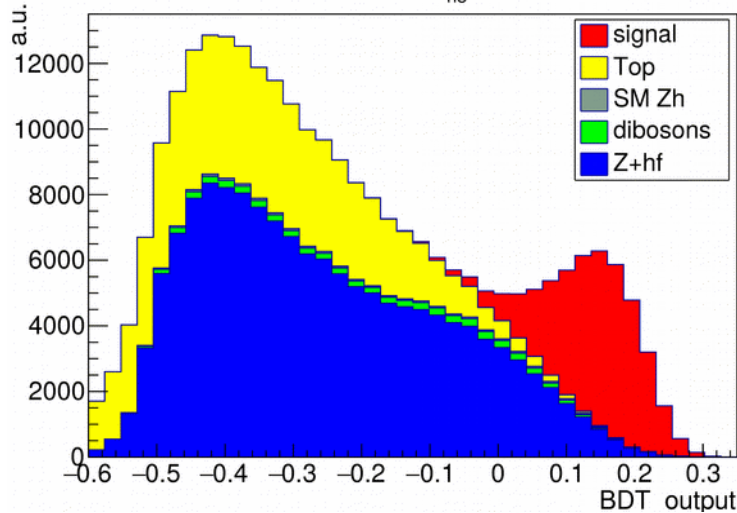
BDT output for $m_{h_2}=400$ GeV



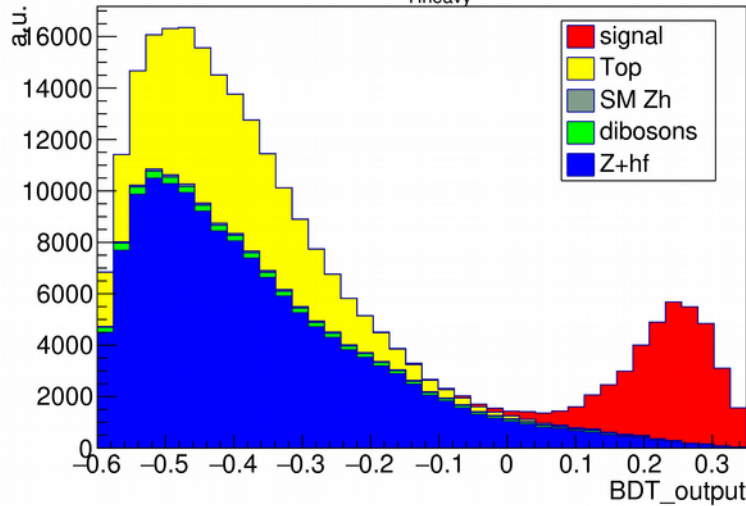
BDT output for $M_{H_{\text{heavy}}}=550$ GeV



BDT output for $m_{h_3}=450$ GeV



BDT output for $M_{H_{\text{heavy}}}=600$ GeV

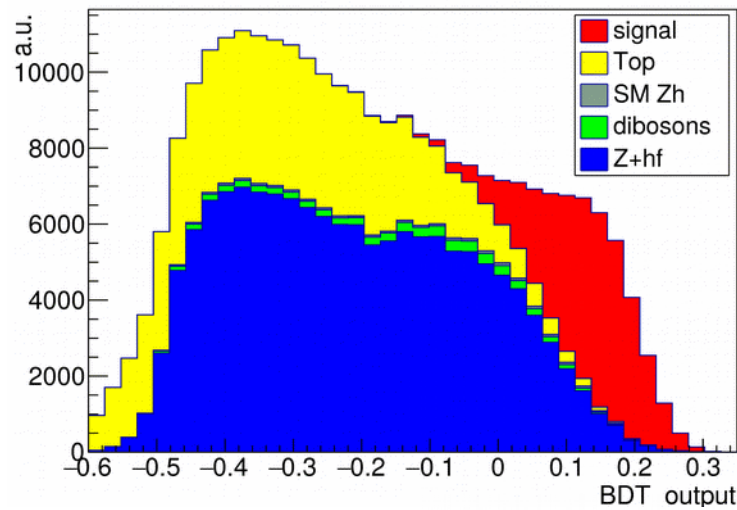


Collider Phenomenology

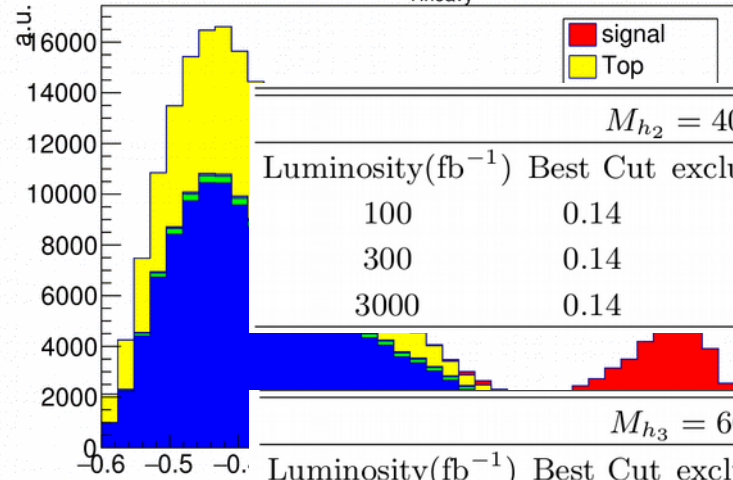
- Distribution for BDT score

$$\sigma(pp \rightarrow h_{2,3})\text{Br}(h_{2,3} \rightarrow Zh_1)\text{Br}(h_1 \rightarrow b\bar{b})$$

BDT output for $m_{h_2}=400$ GeV



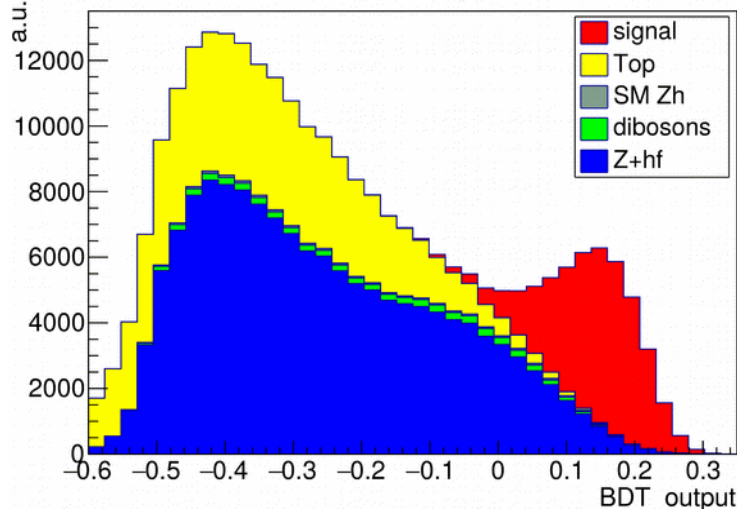
BDT output for $M_{H_{\text{heavy}}}=550$ GeV



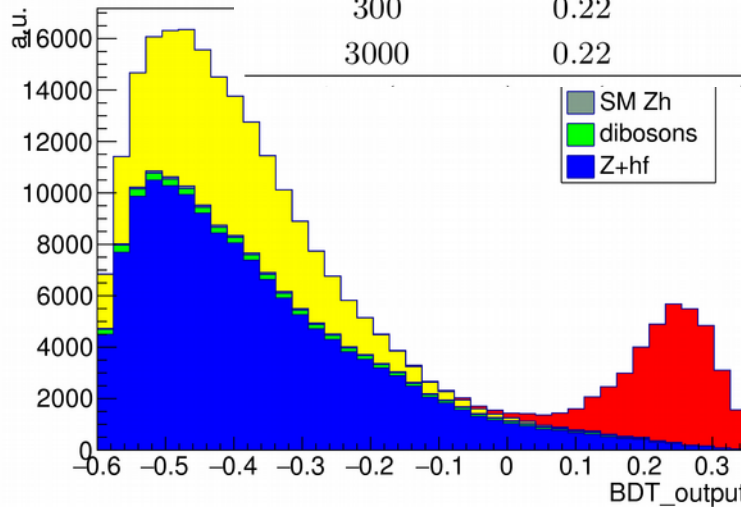
$M_{h_2} = 400$ GeV (14 TeV)			
Luminosity(fb^{-1})	Best Cut	exclusion limit σ_L (pb)	cut-based result (pb)
100	0.14	0.0582	0.1003
300	0.14	0.0336	0.0571
3000	0.14	0.0103	0.0185

$M_{h_3} = 600$ GeV (14 TeV)			
Luminosity(fb^{-1})	Best Cut	exclusion limit σ_L (pb)	cut-based result (pb)
100	0.21	0.0248	0.0340
300	0.22	0.0138	0.0192
3000	0.22	0.00423	0.00598

BDT output for $m_{h_3}=450$ GeV



BD



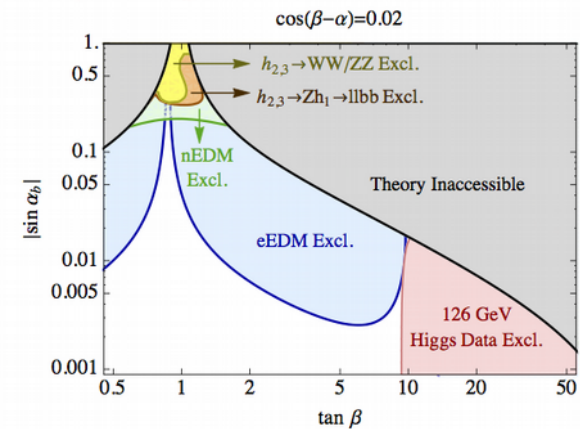
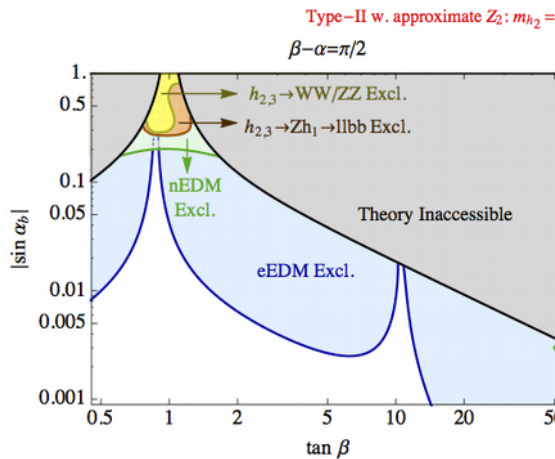
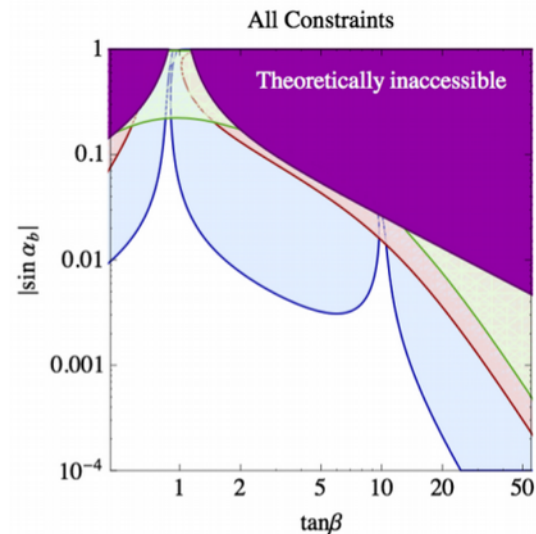
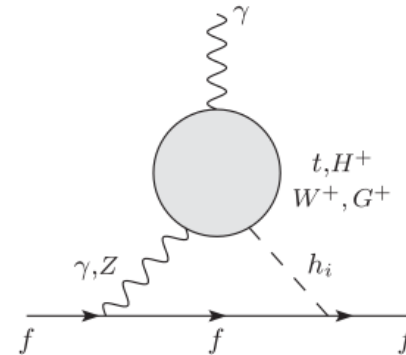
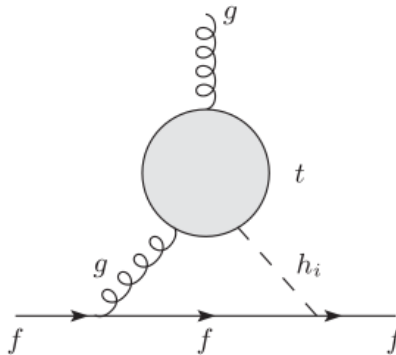
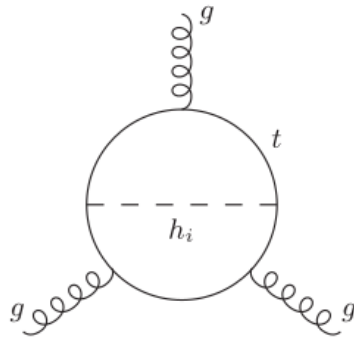
30% to 50% improvements
on upper limit of signal
rate.

EDM limit

- EDM in 2HDM has been studied in

S. Inoue, M. J. Ramsey-Musolf and Y. Zhang, Phys. Rev. D 89, no. 11, 115023 (2014)

L. Bian, T. Liu and J. Shu, Phys. Rev. Lett. 115, 021801 (2015)



C. Y. Chen, S. Dawson and Y. Zhang, JHEP 1506, 056 (2015)

EDM Limit

- EDM limits we take into account:

Source	Current EDM (e cm)	Projected EDM (e cm)
Electron (e)	$d_e < 8.7 \times 10^{-29}$ at 90% CL [15]	$d_e < 8.7 \times 10^{-30}$ [18]
Neutron (n)	$d_n < 2.9 \times 10^{-26}$ at 90% CL [16]	$d_n < 2.9 \times 10^{-28}$ [18]
Mercury (Hg)	$d_{\text{Hg}} < 7.4 \times 10^{-30}$ at 95% CL [48]	-
Radium (Ra)	-	$d_{\text{Ra}} < 10^{-27}$ [18]

Electron: J. Baron et al. [ACME Collaboration], Science 343, 269 (2014)

Neutron: Baker, C. A. et al., Phys. Rev. Lett. 97, 131801 (2006)

Mercury: B. Graner, Y. Chen, E. G. Lindahl and B. R. Heckel, Phys. Rev. Lett. 116, no. 16, 161601 (2016)

Projected: K. Kumar, Z. T. Lu and M. J. Ramsey-Musolf, arXiv:1312.5416

Result

- Two Benchmarks

m_{h_2}	m_{h_3}	m_{H^+}	ν
400 GeV	450 GeV	420 GeV	1
550 GeV	600 GeV	620 GeV	1

They satisfy the Electroweak Precision Data.

Result

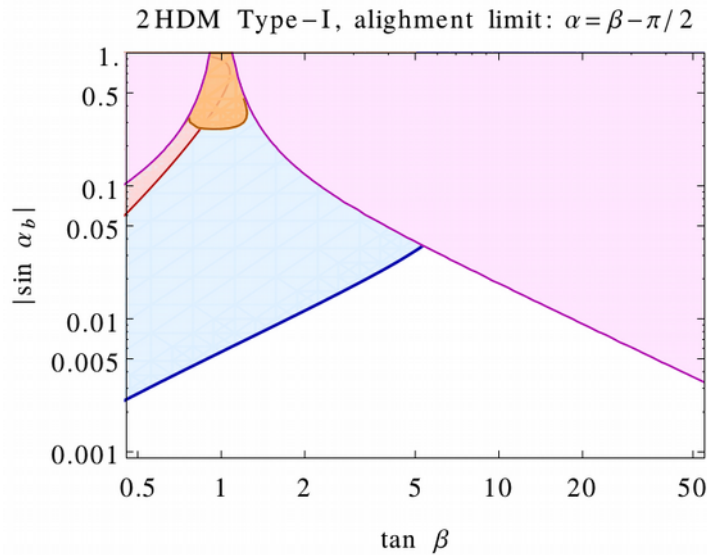
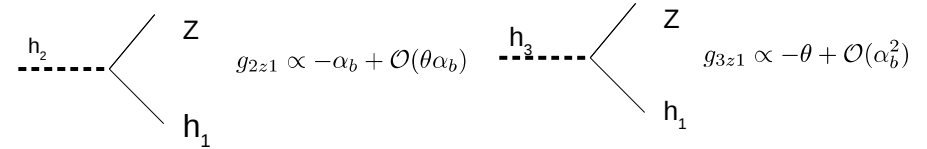
- Two Benchmarks

m_{h_2}	m_{h_3}	m_{H^+}	ν
400 GeV	450 GeV	420 GeV	1
550 GeV	600 GeV	620 GeV	1

They satisfy the Electroweak Precision Data.

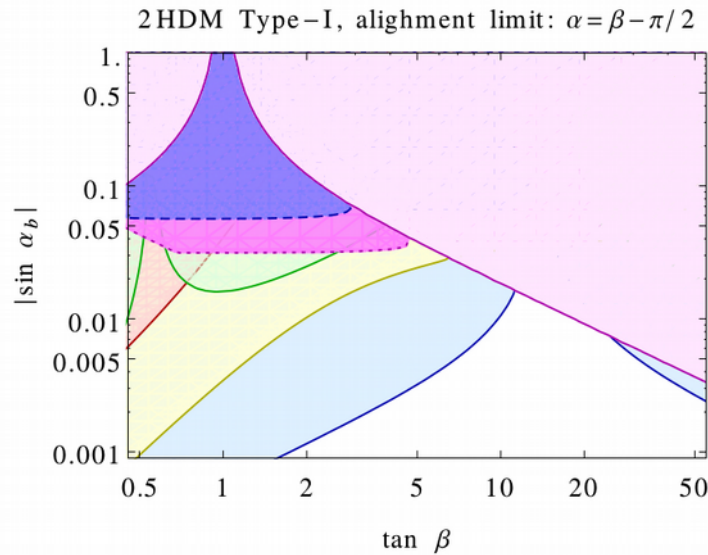
Results

- Alignment limit
Type-I



(a) Type-I Alignment limit current

$$\begin{aligned}
 \tilde{c}_{1,t,b} &= -\alpha_b \cot \beta \\
 \tilde{c}_{2,t,b} &= \alpha_c \cot \beta \\
 \tilde{c}_{3,t,b} &= \cot \beta
 \end{aligned}$$



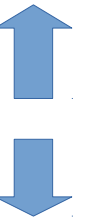
(b) Type-I Alignment limit future

$$\begin{aligned}
 c_{1,t,b} &= 1 & g_{2z1} &= -\alpha_b \\
 c_{2,t,b} &= \cot \beta \\
 c_{3,t,b} &= -\cot \beta & g_{3z1} &= \mathcal{O}(\alpha_b^2)
 \end{aligned}$$

- Theoretical Inaccessible
- Current LHC $A \rightarrow Zh$
- Mercury
- eEDM
- Ra EDM
- neutron EDM
- LHC 14 TeV $0.3 \text{ ab}^{-1/2}$
- LHC 14 TeV $3 \text{ ab}^{-1/2}$

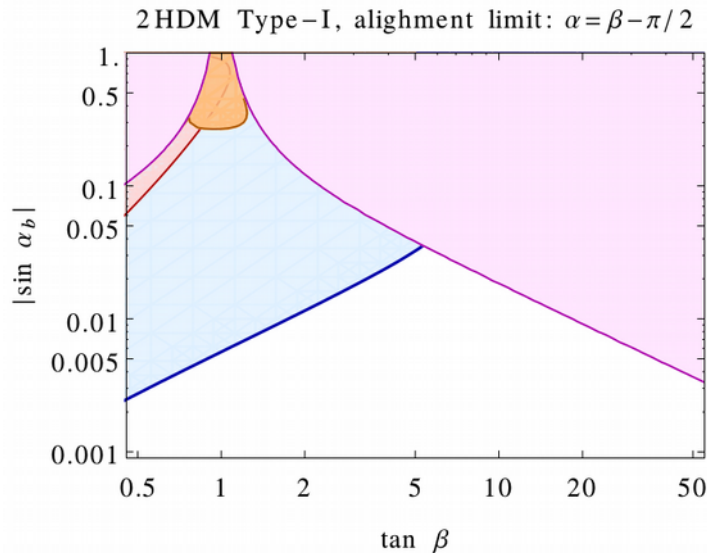
At small $\tan \beta$
 $\sigma(pp \rightarrow h_2)$

$\text{BR}(h_2 \rightarrow Zh_1)$



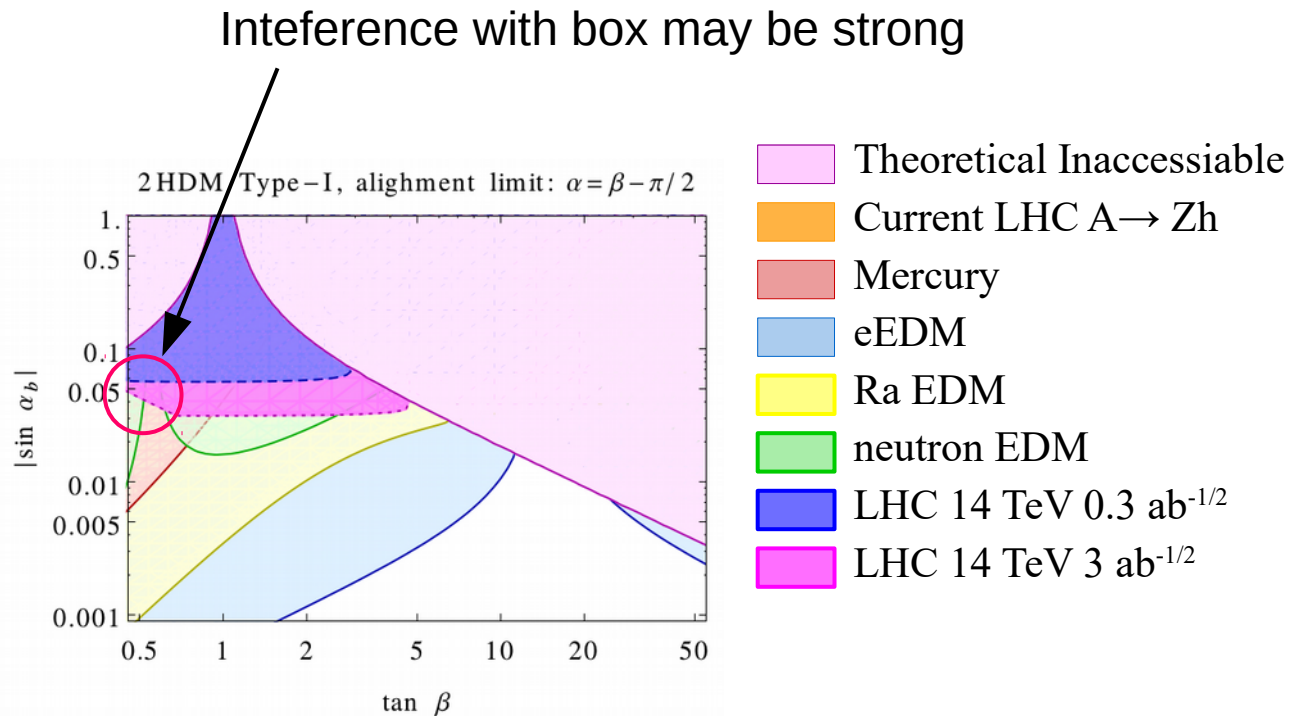
Results

- Alignment limit
Type-I



(a) Type-I Alignment limit current

$$\begin{aligned}\tilde{c}_{1,t,b} &= -\alpha_b \cot \beta \\ \tilde{c}_{2,t,b} &= \alpha_c \cot \beta \\ \tilde{c}_{3,t,b} &= \cot \beta\end{aligned}$$

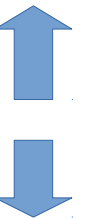


(b) Type-I Alignment limit future

$$\begin{aligned}c_{1,t,b} &= 1 & g_{2z1} &= -\alpha_b \\ c_{2,t,b} &= \cot \beta \\ c_{3,t,b} &= -\cot \beta & g_{3z1} &= \mathcal{O}(\alpha_b^2)\end{aligned}$$

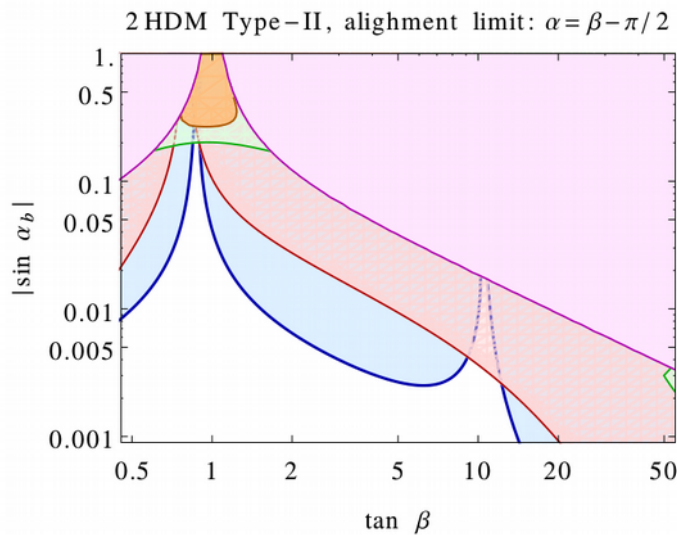
At small $\tan \beta$
 $\sigma(pp \rightarrow h_2)$

$\text{BR}(h_2 \rightarrow Zh_1)$

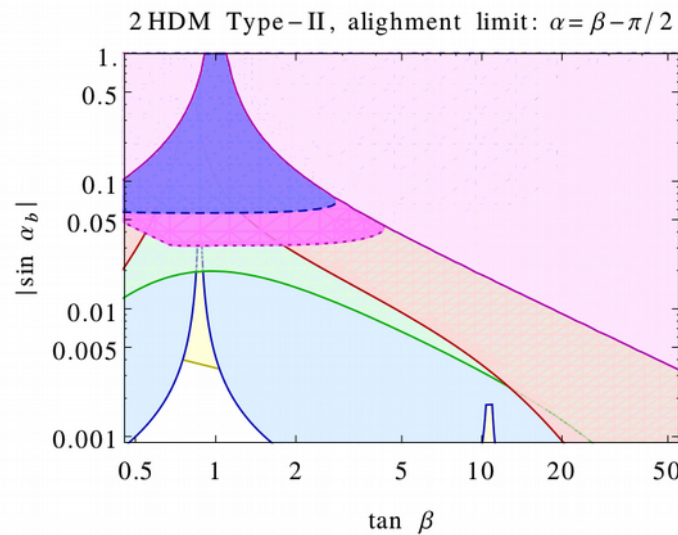


Results

- Alignment limit
Type-II



(a) Type-II Alignment limit current



(b) Type-II Alignment limit future

- Theoretical Inaccessible
- Current LHC $A \rightarrow Zh$
- Mercury
- eEDM
- Ra EDM
- neutron EDM
- LHC 14 TeV $0.3 \text{ ab}^{-1/2}$
- LHC 14 TeV $3 \text{ ab}^{-1/2}$

$$\tilde{c}_{1,b} = -\alpha_b \tan \beta$$

$$\tilde{c}_{2,b} = \alpha_c \tan \beta$$

$$\tilde{c}_{3,b} = \tan \beta$$

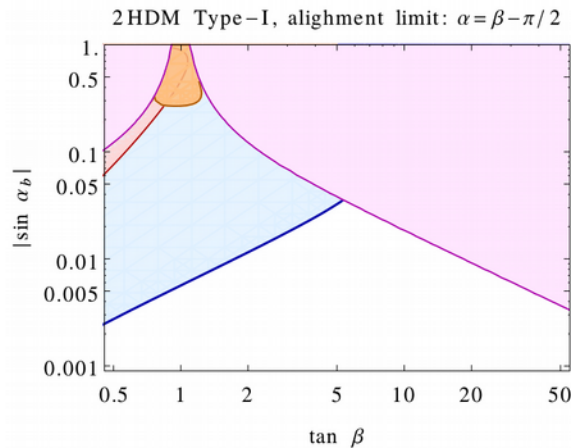
$$c_{1,b} = 1$$

$$c_{2,b} = \tan \beta$$

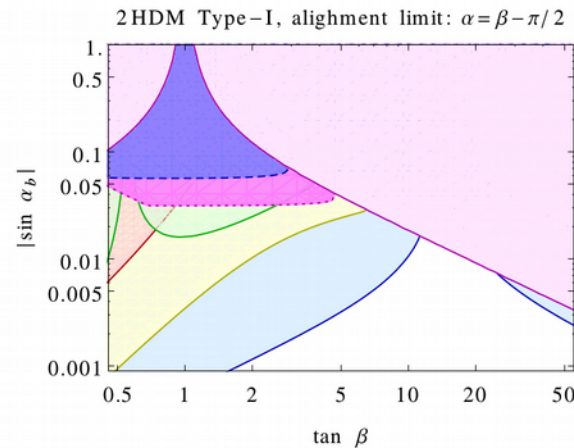
$$c_{3,b} = -\alpha_c \tan \beta - \alpha_b$$

Results

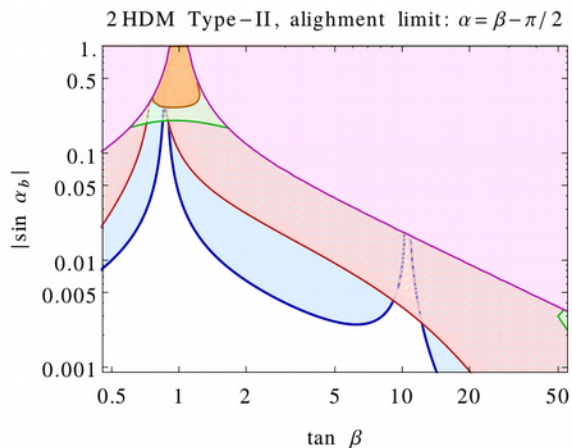
- Summary for the alignment limit



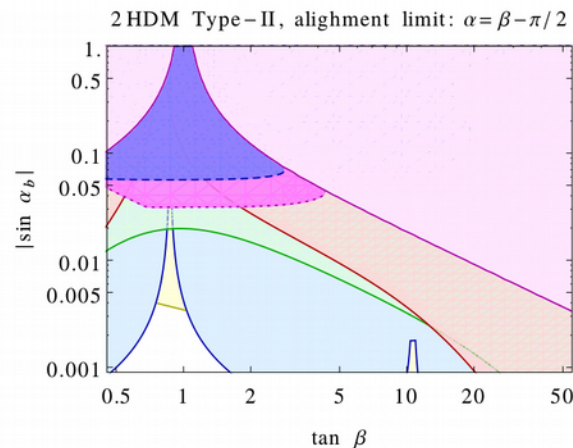
(a) Type-I Alignment limit current



(b) Type-I Alignment limit future



(a) Type-II Alignment limit current



(b) Type-II Alignment limit future

- LHC make a discovery:

Type-I will at least give non-zero
Ra , electron EDM
Otherwise, falsify Type-I.

Type-II will give non-zero
Neutron and Ra EDM
Otherwise, falsify Type-II.

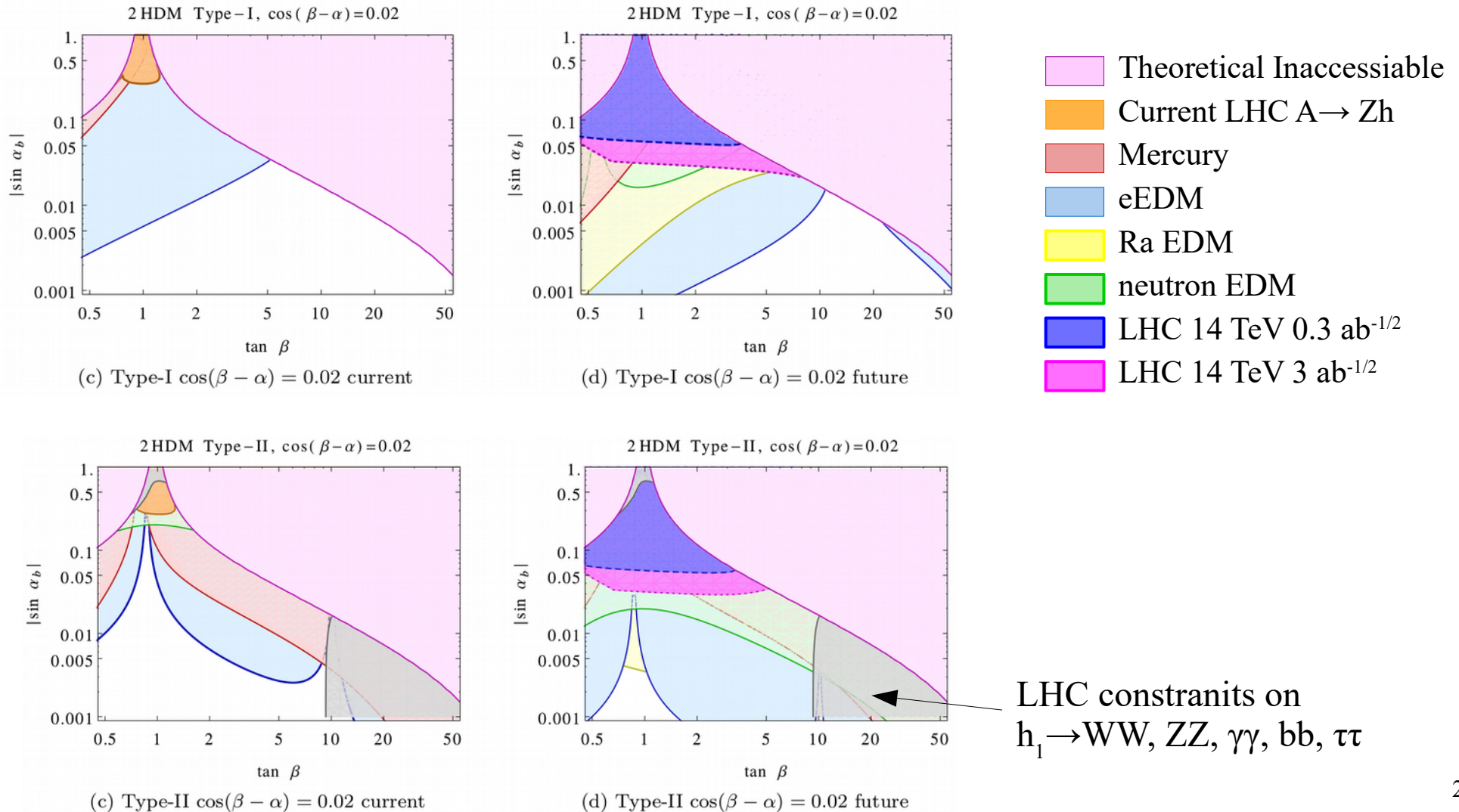
- LHC gives null result:

Does not preclude the possibility for
small CP Violation in 2HDM

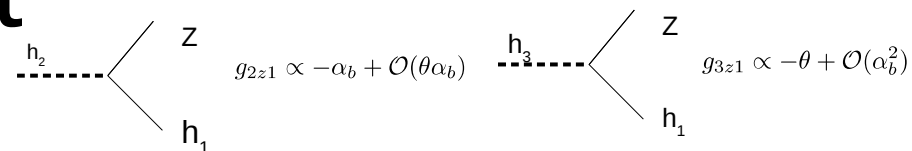
EDM result may or may not falsify
the CPV 2HDM

Result

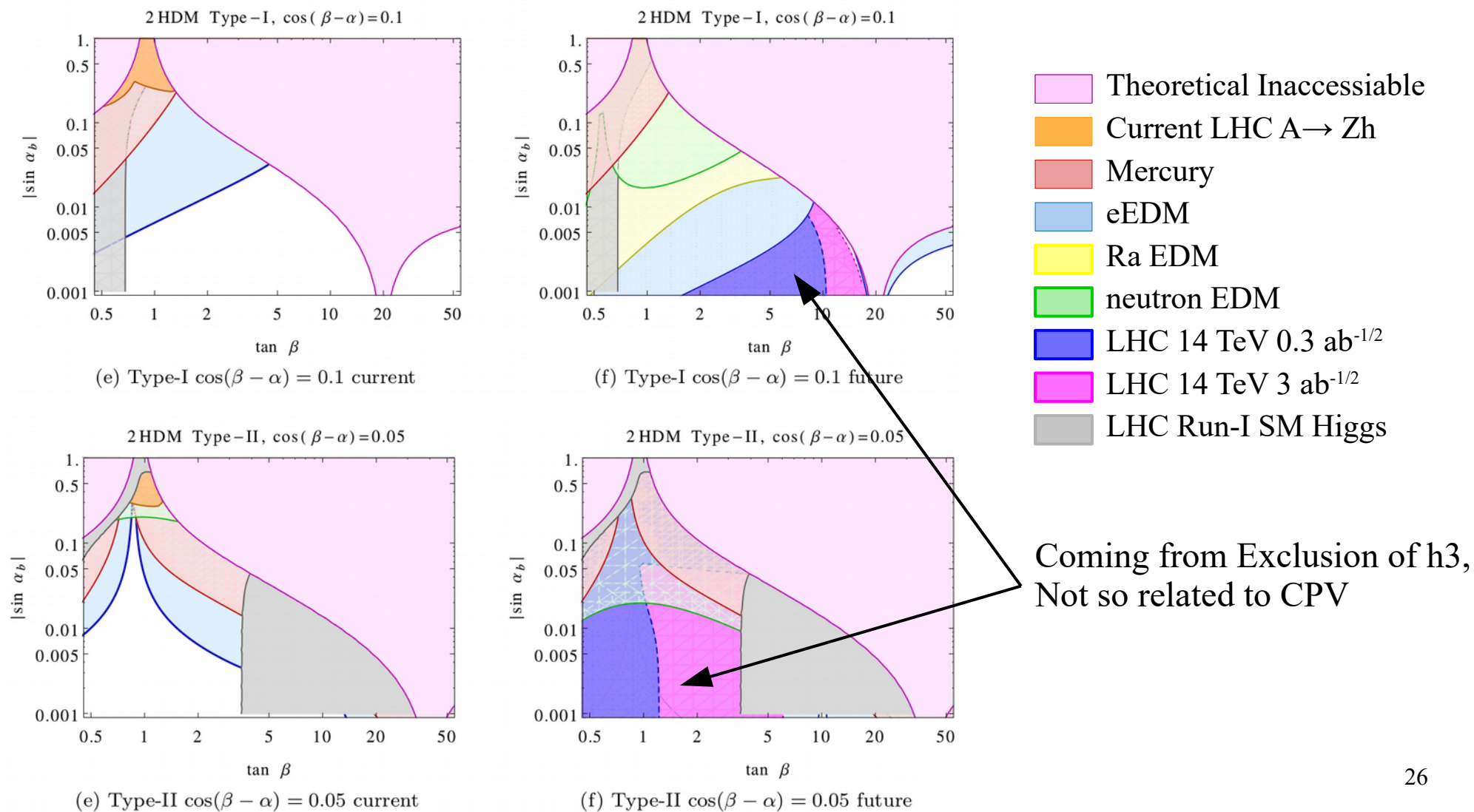
- Small deviation from the alignment limit



Result

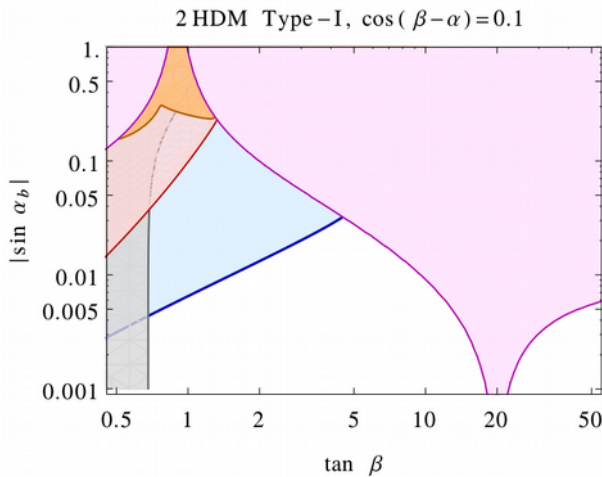


- Large deviation from the alignment limit

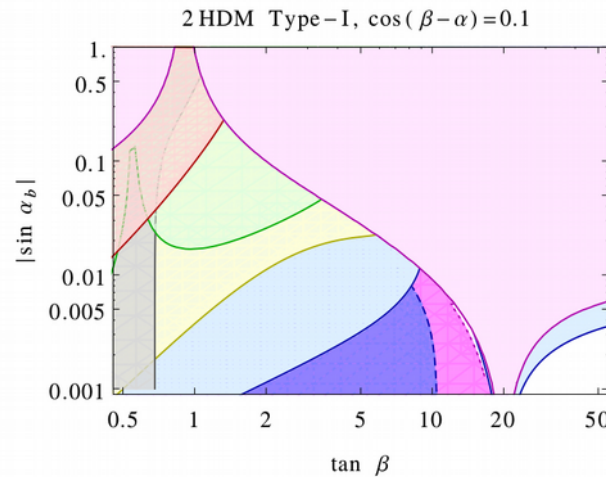


Result

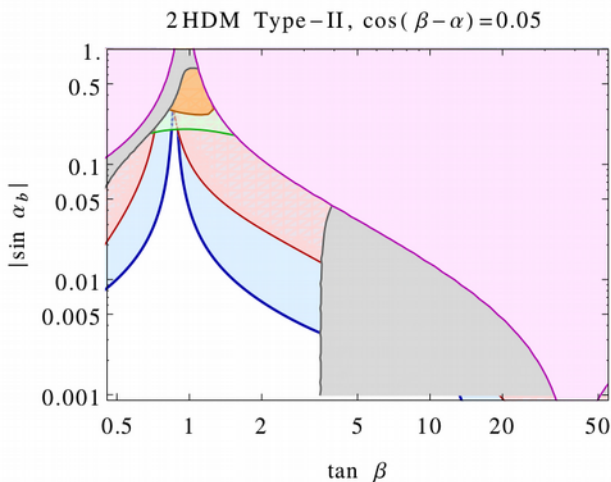
- Large deviation from the alignment limit



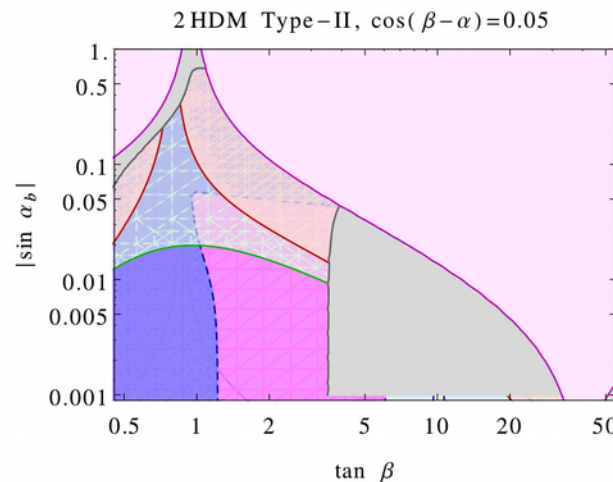
(e) Type-I $\cos(\beta - \alpha) = 0.1$ current



(f) Type-I $\cos(\beta - \alpha) = 0.1$ future



(e) Type-II $\cos(\beta - \alpha) = 0.05$ current



(f) Type-II $\cos(\beta - \alpha) = 0.05$ future

- LHC make a discovery:

One may not conclude that there is a sizeable CPV effect. Need further CP information of the newly discovered particle.

- LHC gives null results:
A non-zero EDM result will falsify CPV 2HDM.

Summary

- Discussed the CPV condition in the 2HDM
- The $h_{23} \rightarrow Zh_1$ is a good process to constraint CP
- EDM experiments will generally better than collider experiments in testing CPV, while the interplay of both experiments will help to falsify CPV 2HDM.

Back up

- Detail of Basis Invariants

$$I_1 = I_3 = 0 \quad \text{due to } \lambda_6 = \lambda_7 = 0$$

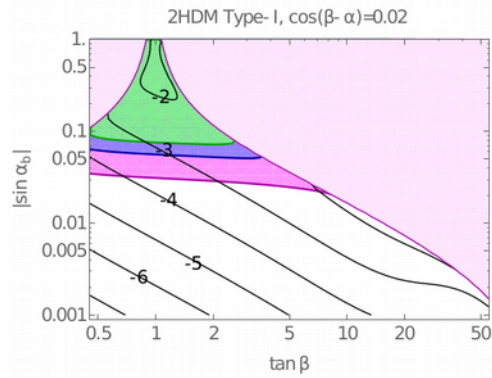
$$I_2 = (\lambda_1 - \lambda_2)[\text{Im}((m_{12}^2)^2 \lambda_5^*)]$$

$$I_4 = 1/2[(\lambda_1 - \lambda_3 - \lambda_4)(\lambda_2 - \lambda_3 - \lambda_4) - |\lambda_5^2|] \\ \times (m_{22}^2 - m_{11}^2) \text{Im}((m_{12}^2)^2 \lambda_5^*)$$

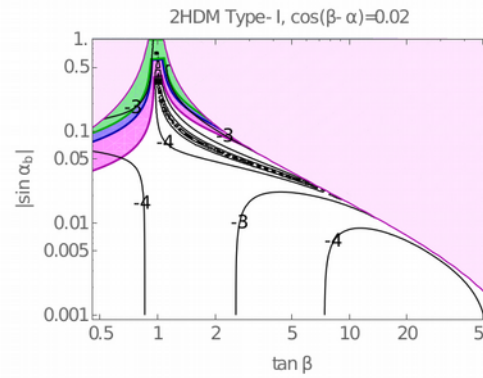
$$J_1 = (\lambda_1 - \lambda_2) \text{Im}(m_{12}^2)$$

$$J_2 = 1/2 v_1 v_2 (v_1 v_2 (m_{11}^4 - m_{22}^4) \text{Im}(\lambda_5) \\ + (m_{11}^2 v_1^2 (\lambda_3 + \lambda_4 - \lambda_1) + m_{22}^2 v_2^2 (\lambda_2 - \lambda_3 - \lambda_4)) \text{Im}(m_{12}^2))$$

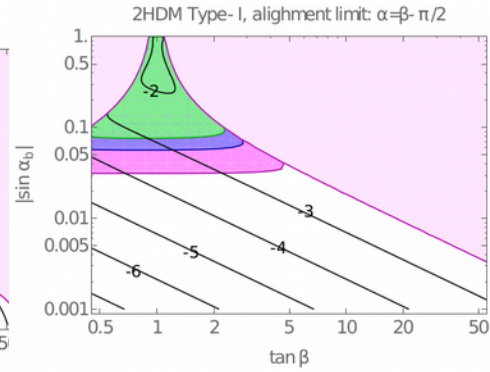
Backup



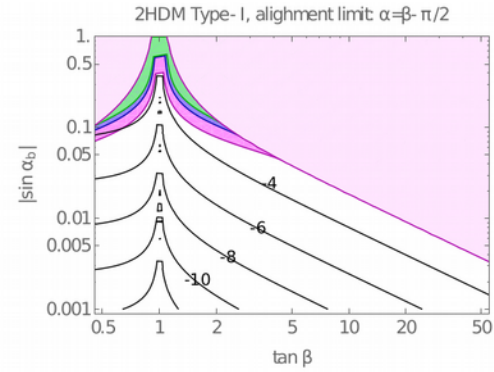
(a) Type-I constraint on h_2



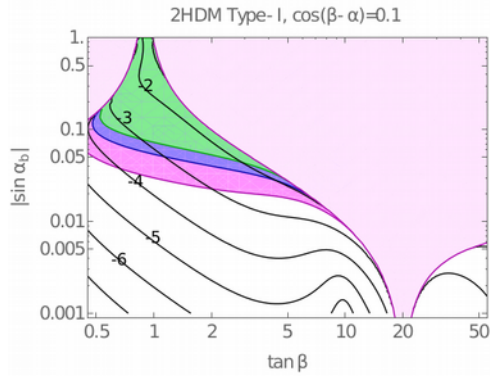
(b) Type-I constraint on h_3



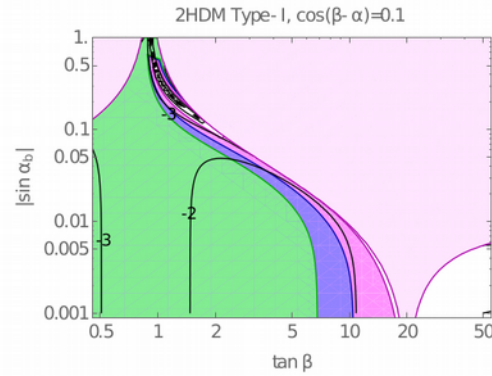
(a) Type-I Alignment limit constraint on h_2



(b) Type-I Alignment limit constraint on h_3



(a) Type-I constraint on h_2



(b) Type-I constraint on h_3

Backup

$$\lambda_1 = \frac{m_{h_1}^2 \sin^2 \alpha \cos^2 \alpha_b + m_{h_2}^2 R_{21}^2 + m_{h_3}^2 R_{31}^2}{v^2 \cos \beta^2} - \nu \tan^2 \beta ,$$

$$\lambda_2 = \frac{m_{h_1}^2 \cos^2 \alpha \cos^2 \alpha_b + m_{h_2}^2 R_{22}^2 + m_{h_3}^2 R_{32}^2}{v^2 \sin \beta^2} - \nu \cot^2 \beta ,$$

$$\text{Re}\lambda_5 = \nu - \frac{m_{h_1}^2 \sin^2 \alpha_b + \cos^2 \alpha_b (m_{h_2}^2 \sin^2 \alpha_c + m_{h_3}^2 \cos^2 \alpha_c)}{v^2} ,$$

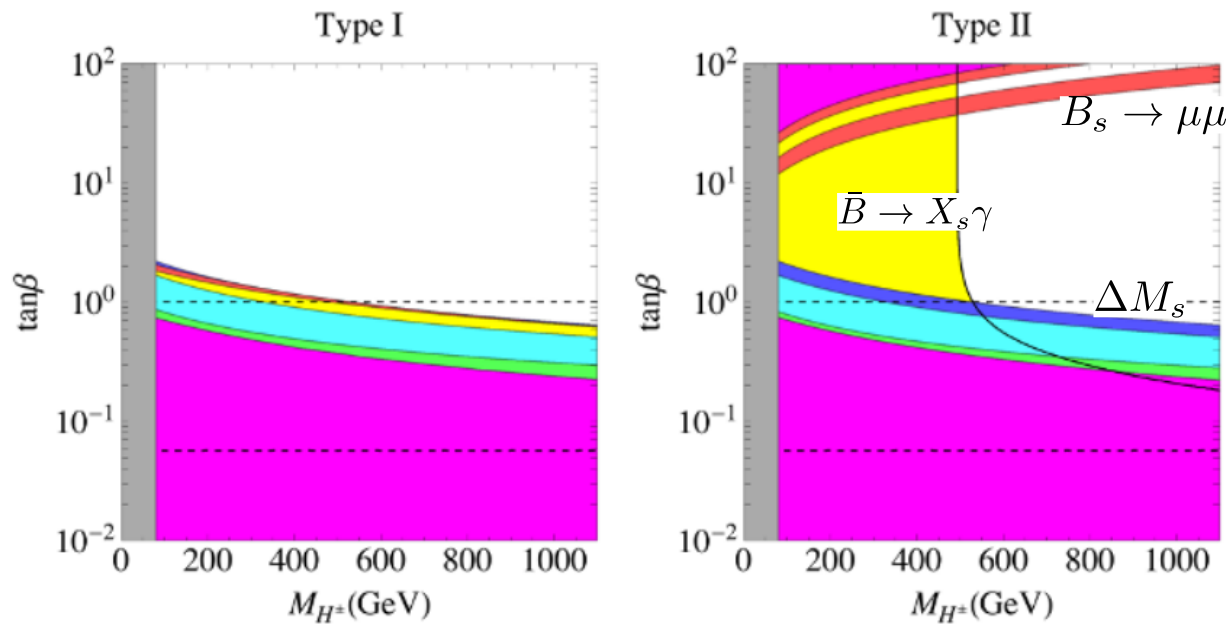
$$\lambda_3 = \nu - \frac{m_{h_1}^2 \sin \alpha \cos \alpha \cos^2 \alpha_b - m_{h_2}^2 R_{21} R_{22} - m_{h_3}^2 R_{31} R_{32}}{v^2 \sin \beta \cos \beta} - \lambda_4 - \text{Re}\lambda_5 ,$$

$$\text{Im}\lambda_5 = \frac{2 \cos \alpha_b [(m_{h_2}^2 - m_{h_3}^2) \cos \alpha \sin \alpha_c \cos \alpha_c + (m_{h_1}^2 - m_{h_2}^2 \sin^2 \alpha_c - m_{h_3}^2 \cos^2 \alpha_c)^2 \sin \alpha \sin \alpha_b]}{v^2 \sin \beta}$$

$$\tan \beta = \frac{(m_{h_2}^2 - m_{h_3}^2) \cos \alpha_c \sin \alpha_c + (m_{h_1}^2 - m_{h_2}^2 \sin^2 \alpha_c - m_{h_3}^2 \cos^2 \alpha_c) \tan \alpha \sin \alpha_b}{(m_{h_2}^2 - m_{h_3}^2) \tan \alpha \cos \alpha_c \sin \alpha_c - (m_{h_1}^2 - m_{h_2}^2 \sin^2 \alpha_c - m_{h_3}^2 \cos^2 \alpha_c) \sin \alpha_b} .$$

Back up

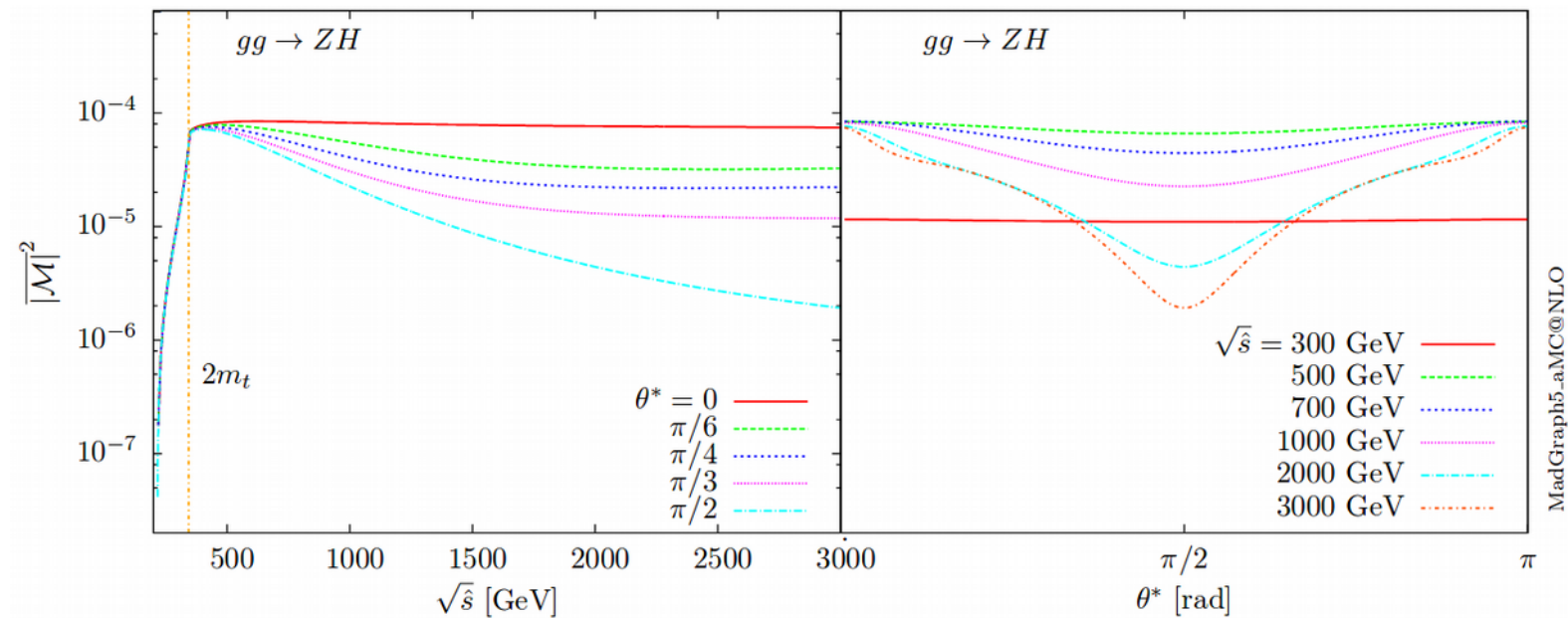
- Flavor Constraint



T. Enomoto and R. Watanabe, J. High Energy Phys. 05(2016) 002.

Backup

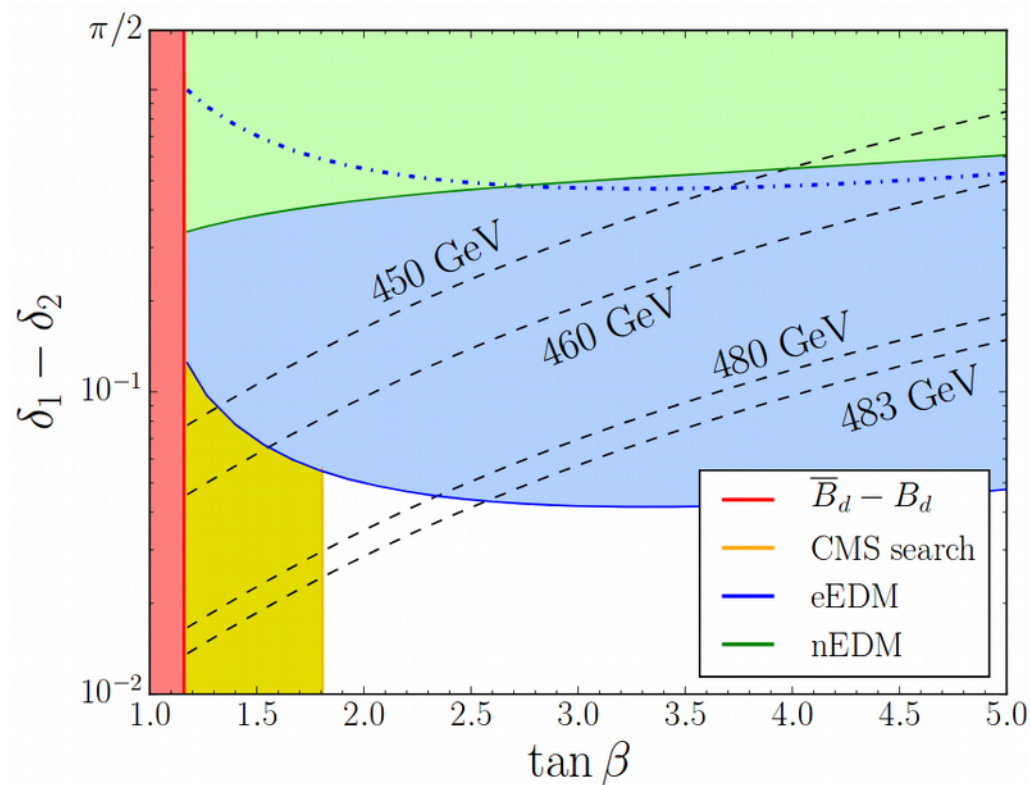
- Box interference



$$|\overline{\mathcal{M}}|_{res,peak}^2 > 10^{-4}$$

Backup

- Relation to Electroweak Baryogenesis



CP Violation 2HDM from collider to EDM

Hao-Lin Li

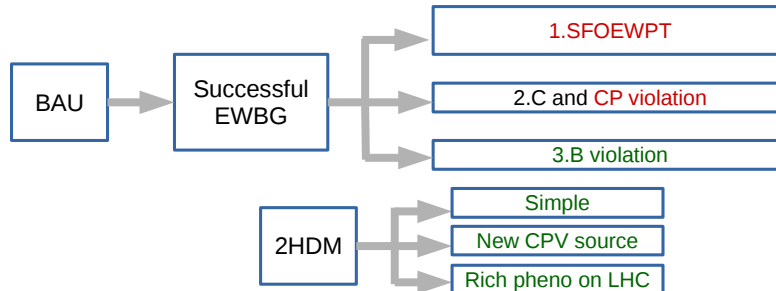
Amherst Center for Fundamental Interaction (ACFI)
University of Massachusetts Amherst

C.-Y. Chen, H.-L. Li, M.J. Ramsey-Musolf, Phys.Rev. D97 (2018) no.1, 015020



Motivation and Goal

- Motivation



- Goal:

Future reach of LHC Testing CPV in Scalar sector
 $p p \rightarrow h_{2,3} \rightarrow Z(l)h(bb)$

Future EDM experiment

Falsify CPV2DHM

2

This is our motivation and goal of this work. The biggest motivation is to try to understand the origin of the baryon asymmetry of our universe. The EWBG is one of the appealing solutions to this problem due to its testability. A successful EWBG needs to satisfy 3 Sakharov conditions. The first is the presence of SFOEWPT. The second condition requires C and CP violation, the third one requires Baryon number violation. In the SM, the B V is processed via EW Sph process. However the effect of CP violation is too feeble and the EWPT is cross-over so that cannot satisfy the first two conditions, new physics must be needed. 2HDM is one of the candidates to solve these problems. The reason we choose 2HDM is that it is one of the simplest extensions to the SM, and it provides a new CP source at Tree level, and furthermore it predicts a rich phenomenology which can be tested in the collider experiments. Our goal is to estimate the ability of future collider experiments in testing CPV in the scalar sector in the 2HDM, and also we will explore how to combine the results from EDM and collider to better falsify CPV 2HDM.

Outline

- Introduction of CPV 2HDM
- Collider Phenomenology
- EDM limit
- Results
- Summary

3

This is the outline of my talk. In the first part I will introduce the our theoretical framework in studying CPV 2HDM.

In the second part I will talk about the collider phenomenology related for testing CPV in the scalar sector and discuss some detail about our simulation and analysis.

In the third part I will briefly review the EDM in the 2HDM

Finally I will combine all the limits and constraint to show the results

General 2HDM

- Lagrangian:

$$\begin{aligned} V(\phi_1, \phi_2) = & -\frac{1}{2} \left[m_{11}^2 (\phi_1^\dagger \phi_1) + \left(m_{12}^2 (\phi_1^\dagger \phi_2) + \text{h.c.} \right) + m_{22}^2 (\phi_2^\dagger \phi_2) \right] \\ & + \frac{\lambda_1}{2} (\phi_1^\dagger \phi_1)^2 + \frac{\lambda_2}{2} (\phi_2^\dagger \phi_2)^2 + \lambda_3 (\phi_1^\dagger \phi_1) (\phi_2^\dagger \phi_2) + \lambda_4 (\phi_1^\dagger \phi_2) (\phi_2^\dagger \phi_1) \\ & + \frac{1}{2} \left[\lambda_5 (\phi_1^\dagger \phi_2)^2 + \lambda_6 (\phi_1^\dagger \phi_2) (\phi_1^\dagger \phi_1) + \lambda_7 (\phi_1^\dagger \phi_2) (\phi_2^\dagger \phi_2) + \text{h.c.} \right] . \end{aligned}$$

4 parameters can be complex and potential to trigger CP violation:

$$m_{12}^2 \quad \lambda_5 \quad \lambda_6 \quad \lambda_7$$

2HDM with Z_2

- Z_2 symmetry: Preventing Tree level FCNC

$$Z_2 : \quad \phi_1 \rightarrow -\phi_1 \quad \phi_2 \rightarrow \phi_2$$

$$Q_L \rightarrow Q_L \quad L \rightarrow L$$

No CPV if exact, so soft break retain non-zero m_{12}^2

Model	u_R	d_R	e_R
Type-I	+	+	+
Type-II	+	-	-
Lepton-Specific	+	+	-
Flipped	+	-	+

Only two parameter can be complex:

$$m_{12}^2 \quad \lambda_5 \quad \lambda_6 = \lambda_7 = 0$$

In our analysis we will restrict our self in a soft breaking Z_2 symmetric model to prevent problematic tree level flavor changing neutral current. With the different assignment of Z_2 charge to higgs doublet fermion fields, there are generally 4 types of model, in our following analysis, we will only concentrate on the type-I and type-II model.

Under the soft Z_2 symmetry breaking λ_6 and $\lambda_7 = 0$ leaving only m_{12}^2 and λ_5 potentially be complex.

2HDM with Z_2

- After EWSB

$$\langle \phi_1 \rangle = \begin{pmatrix} 0 \\ v_1 e^{i\delta_1} \end{pmatrix} \quad \langle \phi_2 \rangle = \begin{pmatrix} 0 \\ v_2 e^{i\delta_2} \end{pmatrix} \quad \tan \beta = v_2/v_1$$

- Subset of $U(2)$ that keeps $\lambda_6 = \lambda_7 = 0$

$$e^{i\psi} \begin{pmatrix} 1 & 0 \\ 0 & e^{i\chi} \end{pmatrix} \quad e^{i\psi} \begin{pmatrix} 0 & 1 \\ e^{i\chi} & 0 \end{pmatrix}$$

absorb the phase in the vev without loose generality

m_{12}^2 and λ_5 are **not Independent** related by the minimization condition of potential:

$$\text{Im}(m_{12}^2) = v_1 v_2 \text{Im}(\lambda_5) \quad \Rightarrow \quad \text{Only one phase related parameter}$$

α_b

6

After electroweak symmetry breaking, the vev of two Higgs doublet can generally be complex, one is free to use a Higgs basis transformation that keeps λ_6 and λ_7 zero to absorb the two phases in the vev without loss of generality. So now there are only two independent phases left in the potential parameters m_{12}^2 and λ_5 , however the tadpole condition will related the imaginary part of these two parameters by this formular, which imply that there is only one parameter related to CPV in our model, later we will see that we encode this CPV information in a mixing angle α_b when diagonalizing the neutral Higgs mass matrix.

2HDM with Z_2

- Changing parameter set

In the unitary gauge:

$$\phi_1 = \begin{pmatrix} -\sin \beta H^+ \\ \frac{1}{\sqrt{2}}(v \cos \beta + H_1^0 - i \sin \beta A^0) \end{pmatrix}, \quad \phi_2 = \begin{pmatrix} \cos \beta H^+ \\ \frac{1}{\sqrt{2}}(v \sin \beta + H_2^0 + i \cos \beta A^0) \end{pmatrix}$$

$$\lambda_1, \lambda_2, \lambda_3, \lambda_4, \text{Im} \lambda_5, \text{Re} \lambda_5, \text{Re} m_{12}^2, \text{Im} m_{12}^2, m_{11}^2, m_{22}^2$$

Minimization
condition (3)



Mass of charge Higgs (1)

Diagonalization of neutral Mass matrix (6)

$$v, \tan \beta, \nu, \alpha, \alpha_b, \alpha_c, m_{h_1}, m_{h_2}, m_{h_3}, m_{h_H^+}$$

$$\nu = \frac{\text{Re} m_{12}^2}{v^2 \sin 2\beta}$$

7

In the unitary gauge one can write down two higgs doublet in this form, where H_1 and H_2 are two CP even Higgs, and A is the CP odd Higgs. One can further change the set of potential parameters to the set of physical parameters using these relations. One of the minimization condition will related $\text{Im} \lambda_5$ and $\text{Im} m_{12}^2$ So finally we will end up with 9 physical parameters.

Among these relation I will particularly mention

2HDM with Z_2

- Changing parameter set
In the unitary gauge:

$$\phi_1 = \begin{pmatrix} -\sin \beta H^+ \\ \frac{1}{\sqrt{2}}(v \cos \beta + H_1^0 - i \sin \beta A^0) \end{pmatrix}, \quad \phi_2 = \begin{pmatrix} \cos \beta H^+ \\ \frac{1}{\sqrt{2}}(v \sin \beta + H_2^0 + i \cos \beta A^0) \end{pmatrix}$$

$$\lambda_1, \lambda_2, \lambda_3, \lambda_4, \text{Im} \lambda_5, \text{Re} \lambda_5, \text{Re} m_{12}^2, \text{Im} m_{12}^2, m_{11}^2, m_{22}^2$$

Minimization
condition (3)



Mass of charge Higgs (1)

Diagonalization of neutral Mass matrix (6)

$$v, \tan \beta, \nu, \alpha, \alpha_b, \alpha_c, m_{h_1}, m_{h_2}, m_{h_3}, m_{h_H}^+$$

$$\nu = \frac{\text{Re} m_{12}^2}{v^2 \sin 2\beta}$$

2HDM with Z_2

- Changing parameter set
In the unitary gauge:

$$\phi_1 = \begin{pmatrix} -\sin \beta H^+ \\ \frac{1}{\sqrt{2}}(v \cos \beta + H_1^0 - i \sin \beta A^0) \end{pmatrix}, \quad \phi_2 = \begin{pmatrix} \cos \beta H^+ \\ \frac{1}{\sqrt{2}}(v \sin \beta + H_2^0 + i \cos \beta A^0) \end{pmatrix}$$

$$\lambda_1, \lambda_2, \lambda_3, \lambda_4, \text{Im} \lambda_5, \text{Re} \lambda_5, \text{Re} m_{12}^2, \text{Im} m_{12}^2, m_{11}^2, m_{22}^2$$

Minimization
condition (3)

Mass of charge Higgs (1)

Diagonalization of neutral Mass matrix (6)

$$v, \tan \beta, \nu, \alpha, \alpha_b, \alpha_c, m_{h_1}, m_{h_2}, m_{h_3}, m_{h_H}^+$$

$$\nu = \frac{\text{Re} m_{12}^2}{v^2 \sin 2\beta}$$

2HDM with Z_2

- Diagonalization of neutral Higgs mass matrix

$$RM_n^2 R^T = \text{diag}(m_{h_1}^2, m_{h_2}^2, m_{h_3}^2) \quad (h_1, h_2, h_3) = (H_1^0, H_2^0, A^0)R$$

$$R = R_{23}(\alpha_c)R_{13}(\alpha_b)R_{12}(\alpha + \pi/2)$$

$$-\frac{\pi}{2} < \alpha_c, \alpha_b, \alpha \leq \frac{\pi}{2}$$

$$M_n^2 = v^2 \begin{pmatrix} \lambda_1 c_\beta^2 + \nu s_\beta^2 & (\lambda_{345} - \nu) c_\beta s_\beta & -\frac{1}{2} \text{Im } \lambda_5 s_\beta \\ (\lambda_{345} - \nu) c_\beta s_\beta & \lambda_2 s_\beta^2 + \nu c_\beta^2 & -\frac{1}{2} \text{Im } \lambda_5 c_\beta \\ -\frac{1}{2} \text{Im } \lambda_5 s_\beta & -\frac{1}{2} \text{Im } \lambda_5 c_\beta & -\text{Re } \lambda_5 + \nu \end{pmatrix}$$

Non-vanishing $\text{Im } \lambda_5$ signals the mixing between CP even and CP odd Higgs, i.e. trigger CP Violation in the scalar sector.

$$\alpha_c = \begin{cases} \alpha_c^-, & \alpha + \beta \leq 0 \\ \alpha_c^+, & \alpha + \beta > 0 \end{cases}, \quad \tan \alpha_c^\pm = \frac{\mp |\sin \alpha_b^{\max}| \pm \sqrt{\sin^2 \alpha_b^{\max} - \sin^2 \alpha_b}}{\sin \alpha_b} \sqrt{\frac{m_{h_3}^2 - m_{h_1}^2}{m_{h_2}^2 - m_{h_1}^2}}.$$

8

In general the neutral Higgs mass matrix can be written in this form, one can clearly see that the non-zero Im part of λ_5 will trigger the mixing between CP even and CP odd Higgs which signals the CP violation in the scalar sector.

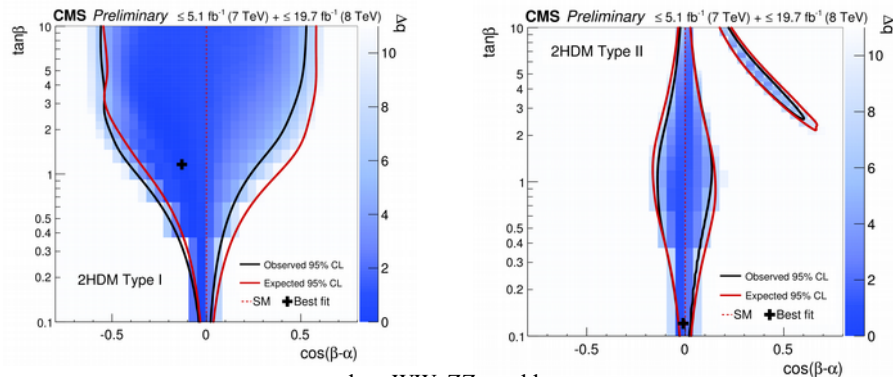
Rotation matrix can be parametrized by three mixing angle α_b , α_c and α . And the higgs mass eigen state is call h_1 , h_2 and h_3 , under this parametrization, when α_b and α_c is small, the h_2 corresponds to the most CP even higgs and h_3 corresponds to the most CP odd Higgs.

α_b and α_c is related to this relation, this expression generate a theoretical bond where one must ensure there is a real solution for α_c .

Collider Phenomenology

Collider Phenomenology

- SM-like Higgs global fit favor alignment limit:



CMS Collaboration, Report No. CMS-PAS-HIG-16-007.

$h_1 \rightarrow WW, ZZ, \gamma\gamma, bb, \tau\tau$

$$\cos(\beta - \alpha) \sim 0$$

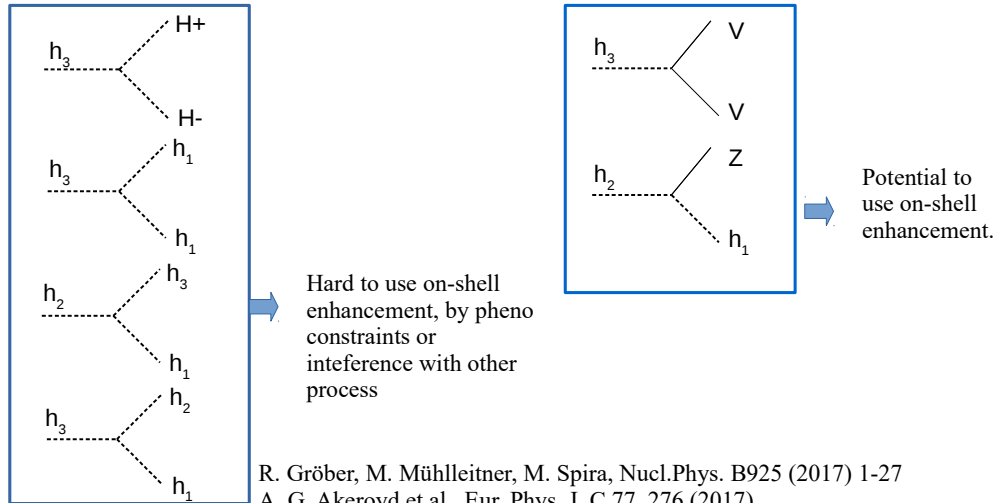
Parametrize the deviation by:

$$\beta - \alpha = \pi/2 + \theta$$

The first concept I would like to discuss is the so called alignment limit, which denoted by $\cos\beta-\alpha=0$, in the CPC 2HDM, under this condition the coupling between SM like Higgs and other SM particles like vector boson become their SM values automatically without setting the mass of heavy higgs to infinity. This is where the words “alignment” come from. This is the global fit for the Higgs signal strength from LHC run-I results. One can observe that in the Type-II model, the absolute value of $\cos\beta-\alpha$ is strongly constrict to the alignment limit. In spite of the possibility that in the Type-I model the deviation from the alignment limit can be large at large $\tan\beta$. In the following analysis we focus on the case of small deviation, and we parametrize the small deviation by a small parameter θ .

Collider Phenomenology

- Possible new channel sensitive to CP violation



R. Gröber, M. Mühlleitner, M. Spira, Nucl.Phys. B925 (2017) 1-27
 A. G. Akeroyd et al., Eur. Phys. J. C 77, 276 (2017)
 C. Y. Chen, S. Dawson and Y. Zhang, JHEP 1506, 056 (2015)

10

Here we list the several three point vertices that are potentially be used to probe the CPV in the scalar sector in the collider experiments. The vertices in the left column are generally hard to use on-shell enhancement due to either phenomenological constraint or submerged by large non-resonant process with the same final state.

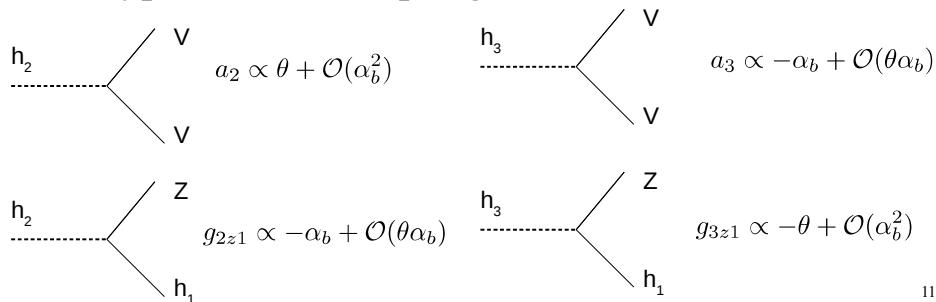
While the diagram on the right will be able to take the advantage of the onshell enhancement, which is studied by this literature.

2HDM with Z_2

- Higgs couplings:

$$\begin{aligned}\mathcal{L}_{int} = & -\frac{m_f}{v} h_i (c_{f,i} \bar{f} f + \tilde{c}_{f,i} \bar{f} i \gamma_5 f) \\ & + a_i h_i \left(\frac{2m_W^2}{v} W_\mu W^\mu + \frac{m_Z^2}{v} Z_\mu Z^\mu \right) \\ & + g_{iz1} Z^\mu ((\partial_\mu h_i) h_1 - h_i \partial_\mu h_1)\end{aligned}$$

Two types of new couplings:



11

Now let's take a closer look of the coupling related to these two channels that are possible to take advantage of on-shell enhancement. We denote a_i are the couplings between the higgs and vector boson, g_{iz1} are the coupling between heavy higgs and $z h$. One can expand these couplings in the small θ violation angle limit and also small deviation from the alignment limit. It is significant to notice that the $h_2 z h$ coupling is directly sensitive to the θ violation angle while the h_3 to $z h$ coupling is sensitive to the deviation from the alignment limit. Later we will only focus on these two processes. This is the most important slides in my talk.

2HDM with Z_2

- Higgs couplings:

$$\begin{aligned}\mathcal{L}_{int} = & -\frac{m_f}{v} h_i (c_{f,i} \bar{f} f + \tilde{c}_{f,i} \bar{f} i \gamma_5 f) \\ & + a_i h_i \left(\frac{2m_W^2}{v} W_\mu W^\mu + \frac{m_Z^2}{v} Z_\mu Z^\mu \right) \\ & + g_{iz1} Z^\mu ((\partial_\mu h_i) h_1 - h_i \partial_\mu h_1)\end{aligned}$$

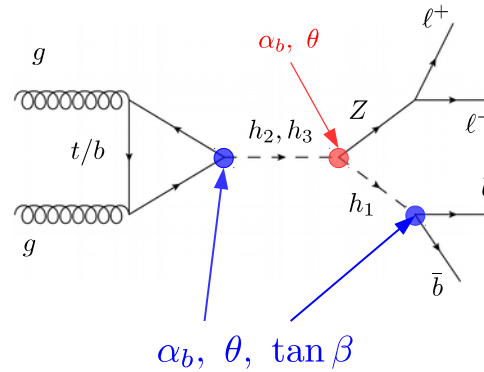
Two types of new couplings:

$$\begin{array}{cc} \begin{array}{c} \text{h}_2 \text{---} \diagup \text{V} \\ \text{---} \diagdown \text{V} \end{array} & a_2 \propto \theta + \mathcal{O}(\alpha_b^2) \end{array} \quad \begin{array}{cc} \begin{array}{c} \text{h}_3 \text{---} \diagup \text{V} \\ \text{---} \diagdown \text{V} \end{array} & a_3 \propto -\alpha_b + \mathcal{O}(\theta \alpha_b) \end{array}$$

$$\begin{array}{cc} \begin{array}{c} \text{h}_2 \text{---} \diagup \text{Z} \\ \text{---} \diagdown \text{h}_1 \end{array} & g_{2z1} \propto -\alpha_b + \mathcal{O}(\theta \alpha_b) \end{array} \quad \begin{array}{cc} \begin{array}{c} \text{h}_3 \text{---} \diagup \text{Z} \\ \text{---} \diagdown \text{h}_1 \end{array} & g_{3z1} \propto -\theta + \mathcal{O}(\alpha_b^2) \end{array}$$

Collider Phenomenology

- In the following we will focus on the process



Derive the prospective upper limit on
 $\sigma(pp \rightarrow h_{2,3})\text{Br}(h_{2,3} \rightarrow Zh_1)\text{Br}(h_1 \rightarrow b\bar{b})$
 in future 14TeV LHC and project this limit onto the
 $|\sin\alpha_b|$ vs $\tan\beta$

12

I will focus on this particular channel in the following analysis and derive the prospective upper limit on this quantity in future HL LHC. We search for the production of heavy Higgs in gluon fusion mode, with the heavy Higgs decay to Z and h1, and subsequently decay two leptons and two b quark final state. In this process, this coupling is sensitive to CP violation angle α_b and the θ that parametrize the deviation from the alignment limit, these two couplings are sensitive to α_b , θ and also $\tan\beta$. We will see in the following analysis how the combination of these three couplings influence our final results.

Collider Phenomenology


- ATLAS 8TeV analysis revisit ($p p \rightarrow A \rightarrow Z(\ell\ell)h(bb)$)
- 2e or 2 opposite sign μ , with $P_t > 7$ GeV and $|\eta_e|(|\eta_\mu|) < 2.5(2.7)$,
- Exactly 2 b tagged jets, with $P_{T,b}^{\text{lead}} > 45$ GeV and $P_{T,b}^{\text{sub}} > 20$ GeV,
- $83 < m_{\ell\ell} < 95$, and $95 < m_{bb} < 135$.
- $E_{T^{\text{miss}}}/\sqrt{H_T} < 3.5 \text{ GeV}^{1/2}$
- $P_T^Z > 0.44 M_{h2,3} - 106 \text{ GeV}$

ATLAS Collaboration Phys.Lett. B744 (2015) 163-183

13

Before derive the projected limit in 14 TeV. We first try to reproduce the ATLAS 8TeV result to calibrate our monte carlo simulation. These are the cuts used in the ATLAS analysis

Collider Phenomenology



- ATLAS 8TeV analysis revisit
- 2e or 2 opposite sign μ , with $P_t > 7$ GeV and $|\eta_e|(|\eta_\mu|) < 2.5(2.7)$,
- Exactly 2 b tagged jets, with $P_{T,b}^{\text{lead}} > 45$ GeV and $P_{T,b}^{\text{sub}} > 20$ GeV,
- $83 < m_{ll} < 95$, and $95 < m_{bb} < 135$.  Reduce diboson background
- $E_{T^{\text{miss}}}/\sqrt{H_T} < 3.5$ GeV^{1/2}
- $P_T^Z > 0.44 M_{h_{2,3}} - 106$ GeV

ATLAS Collaboration Phys.Lett. B744 (2015) 163-183

14

We demand this quantity less than 3.5, where H_t is the scalar sum of the pt of all the object in the final state. Finally we demand the PT of the reconstructed Z boson to be large then a value depend on the reconstructed invariant mass of the heavy higgs.

Collider Phenomenology

- ATLAS 8TeV analysis revisit
- 2e or 2 opposite sign μ , with $P_t > 7$ GeV and $|\eta_e|(|\eta_\mu|) < 2.5(2.7)$,
- Exactly 2 b tagged jets, with $P_{T,b}^{\text{lead}} > 45$ GeV and $P_{T,b}^{\text{sub}} > 20$ GeV,
- $83 < m_{ll} < 95$, and $95 < m_{bb} < 135$.  Reduce diboson background
- $E_{T^{\text{miss}}}/\sqrt{H_T} < 3.5 \text{ GeV}^{1/2}$  Reduce ttbar background
- $P_{T^Z} > 0.44 M_{h_{2,3}} - 106$ GeV

Collider Phenomenology

- ATLAS 8TeV analysis revisit
- 2e or 2 opposite sign μ , with $P_t > 7$ GeV and $|\eta_e|(|\eta_\mu|) < 2.5(2.7)$,
- Exactly 2 b tagged jets, with $P_{T,b}^{\text{lead}} > 45$ GeV and $P_{T,b}^{\text{sub}} > 20$ GeV,
- $83 < m_{ll} < 95$, and $95 < m_{bb} < 135$. ← Reduce diboson background
- $E_{T^{\text{miss}}}/\sqrt{H_T} < 3.5 \text{ GeV}^{1/2}$ ← Reduce ttbar background
- $P_T^Z > 0.44 M_{h_{2,3}} - 106 \text{ GeV}$ ← Reduce Zbb and SM Zh background

Collider Phenomenology

- Comparasion between ATLAS result and ours

Madgraph, Pythia, Delphes

Backgrounds/ Signal	$\sigma(\text{pb})$	$\sigma \times \int \mathcal{L}$	simulated # of events after cuts	# of expected event in Ref. 30	$A \times \epsilon$
$Z(\ell\ell)bb$	12.91	2.620×10^5	1,788	1443 ± 60	6.825×10^{-3}
$t(bl\nu)\bar{t}(bl\nu)$	18.12	3.678×10^5	359	317 ± 28	9.761×10^{-4}
SM $Z(\ell\ell)h(bb)$	0.02742	5.566×10^2	47	31 ± 1.8	8.443×10^{-2}
Diboson($Z(\ell\ell)Z(bb)$)	0.2122	4.308×10^3	28	30 ± 5	6.679×10^{-3}

Two major Backgrounds

C.-Y. Chen, H.-L. Li, M.J. Ramsey-Musolf, Phys.Rev. D97 (2018) no.1, 015020

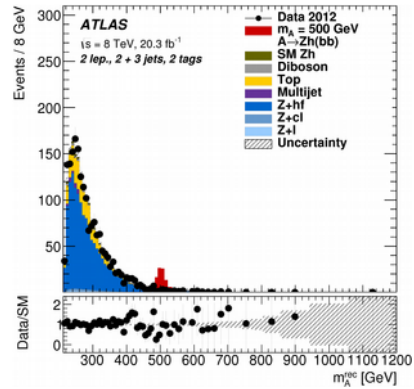
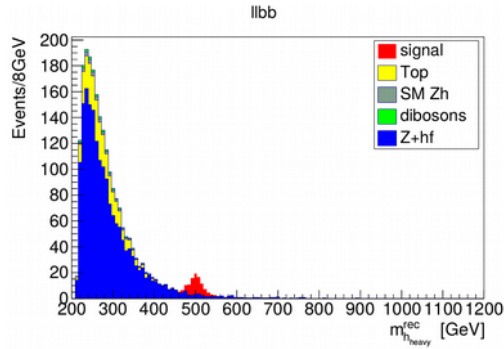
15

We use this cut obtained the similar results in the ATLAS paper

We simulate these four backgrounds using Madgraph, pythia and Delphes. This coluum is the result from our simulation, this coluum is the result estimated by ATLAS group. We can see that our result generally matches the ATLAS results, with a slight more Zbb background

Collider Phenomenology

- Comparasion between ATLAS result and ours

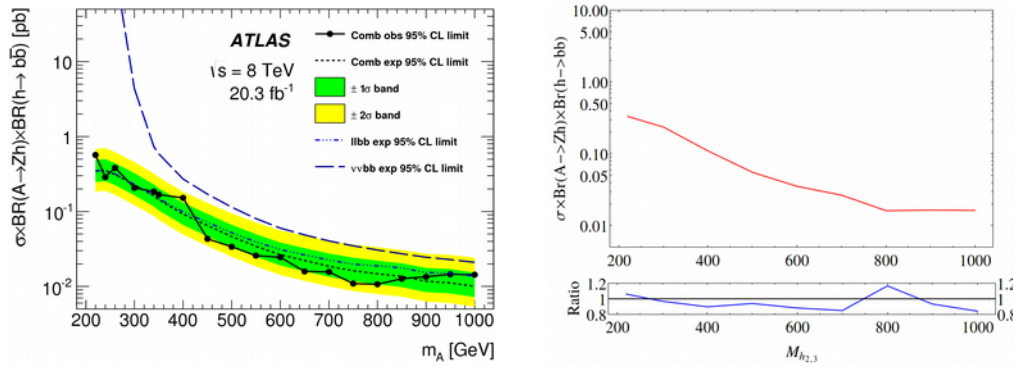


ATLAS Collaboration Phys.Lett. B744 (2015) 163-183

C.-Y. Chen, H.-L. Li, M.J. Ramsey-Musolf, Phys.Rev. D97 (2018) no.1, 015020

Collider Phenomenology

- ATLAS 8TeV analysis revisit



We reproduce the ATLAS results very well.

ATLAS Collaboration Phys.Lett. B744 (2015) 163-183
C.-Y. Chen, H.-L. Li, M.J. Ramsey-Musolf, Phys.Rev. D97 (2018) no.1, 015020

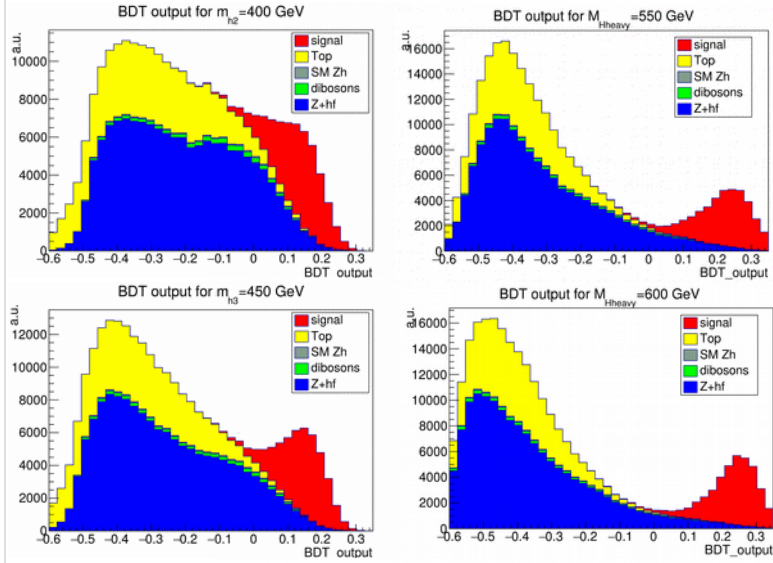
Collider Phenomenology

- 14 TeV forecast
- First select two leptons and two b tagged jets with same kinematic cuts:
- 2e or 2 opposite sign μ , with $P_t > 7$ GeV and $|\eta_e|(|\eta_\mu|) < 2.5(2.7)$,
- Exactly 2 b tagged jets, with $P_{T,b}^{\text{lead}} > 45$ GeV and $P_{T,b}^{\text{sub}} > 20$ GeV,
- Then we compute following quantities as inputs for Boosted Decision Tree(BDT) to optimize the selection.

$$p_{T,\ell}^{\text{lead}}, p_{T,\ell}^{\text{sub}}, p_{T,b}^{\text{lead}}, p_{T,b}^{\text{sub}}, m_{\ell\ell}, m_{bb}, p_T^Z, p_T^h, E_T^{\text{miss}} / \sqrt{H_T}, \Delta R_{\ell\ell}, \Delta R_{jj}, \Delta R_{Zh}, \Delta\phi_{Zh},$$

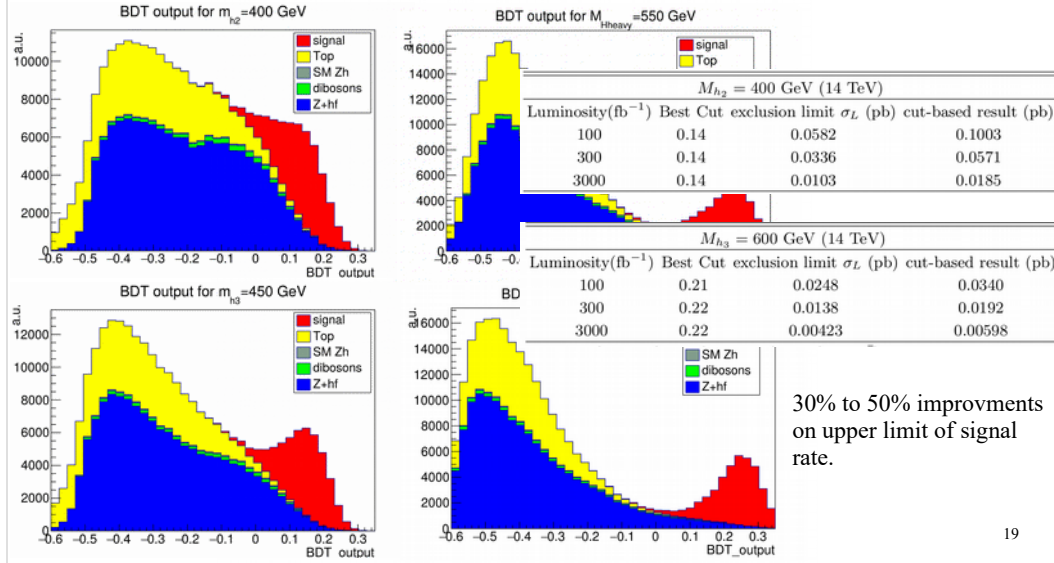
Collider Phenomenology

- Distribution for BDT score



Collider Phenomenology

- Distribution for BDT score $\sigma(pp \rightarrow h_{2,3})\text{Br}(h_{2,3} \rightarrow Zh_1)\text{Br}(h_1 \rightarrow b\bar{b})$

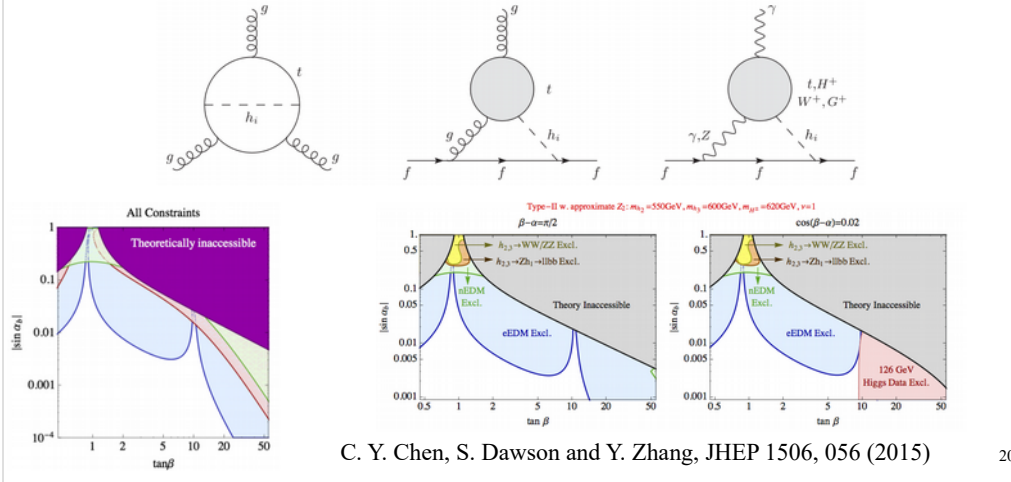


Next we find a cut on the BDT score to obtain the optimized upper limit on this quantity. We find that the BDT analysis generally give 30% to 50% improvement.

EDM limit

- EDM in 2HDM has been studied in

S. Inoue, M. J. Ramsey-Musolf and Y. Zhang, Phys. Rev. D 89, no. 11, 115023 (2014)
L. Bian, T. Liu and J. Shu, Phys. Rev. Lett. 115, 021801 (2015)



20

In general the EDM is generated by these three kinds. It is found that, for the electron EDM, There is cancellation between the barr-zee diagram around $\tan\beta = 1$ in the type-II model. That means the EDM experiments are not sensitive to the test of the CPV in the 2HDM in this region. This is the reason that this paper propose the collider experiment as a complementary to EDM experiments to help to close up the parameter space in this region.

EDM Limit

- EDM limits we take into account:

Source	Current EDM (e cm)	Projected EDM (e cm)
Electron (e)	$d_e < 8.7 \times 10^{-29}$ at 90% CL 15	$d_e < 8.7 \times 10^{-30}$ 18
Neutron (n)	$d_n < 2.9 \times 10^{-26}$ at 90% CL 16	$d_n < 2.9 \times 10^{-28}$ 18
Mercury (Hg)	$d_{\text{Hg}} < 7.4 \times 10^{-30}$ at 95% CL 48	-
Radium (Ra)	-	$d_{\text{Ra}} < 10^{-27}$ 18

Electron: J. Baron et al. [ACME Collaboration], Science 343, 269 (2014)

Neutron: Baker, C. A. et al., Phys. Rev. Lett. 97, 131801 (2006)

Mercury: B. Graner, Y. Chen, E. G. Lindahl and B. R. Heckel, Phys. Rev. Lett. 116, no. 16, 161601 (2016)

Projected: K. Kumar, Z. T. Lu and M. J. Ramsey-Musolf, arXiv:1312.5416

Result

- Two Benchmarks

m_{h_2}	m_{h_3}	m_{H^+}	ν
400 GeV	450 GeV	420 GeV	1
550 GeV	600 GeV	620 GeV	1

They satisfy the Electroweak Precision Data.

Result

- Two Benchmarks

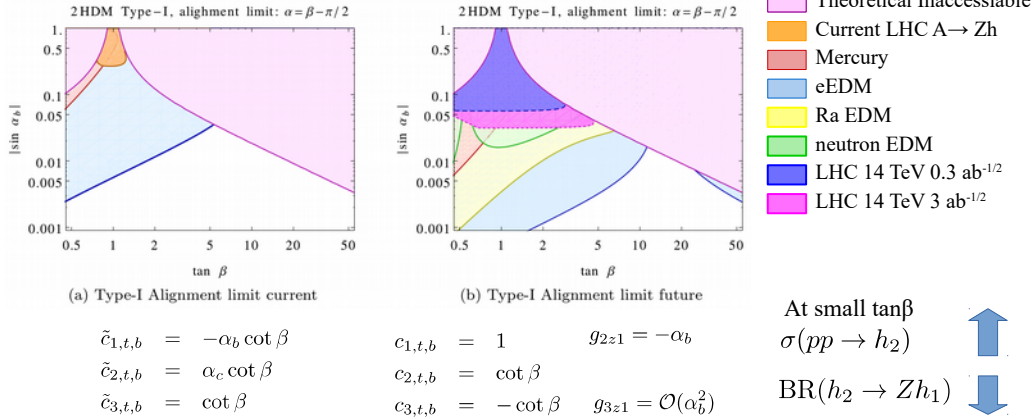
m_{h_2}	m_{h_3}	m_{H^+}	ν
400 GeV	450 GeV	420 GeV	1
550 GeV	600 GeV	620 GeV	1

They satisfy the Electroweak Precision Data.

Results

- Alignment limit
Type-I

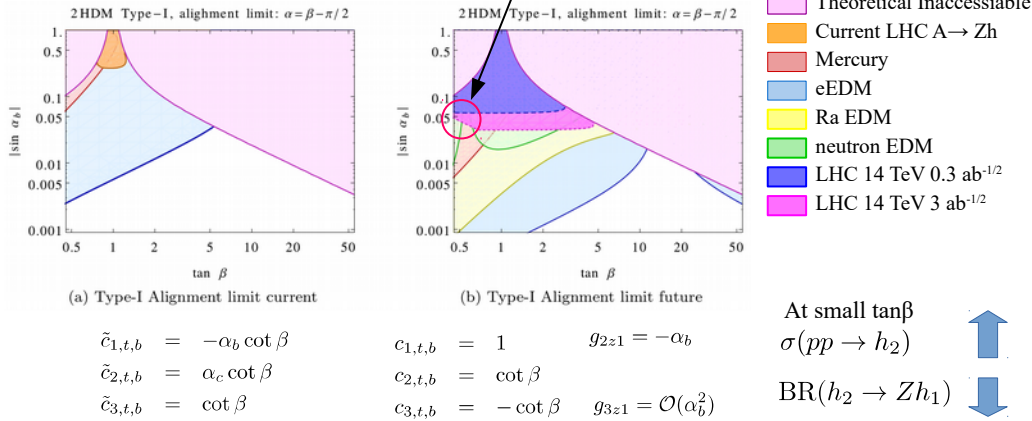
$$\begin{array}{c}
 h_2 \text{---} \swarrow \quad \searrow \quad \text{Z} \\
 \quad \quad \quad h_1 \quad \quad \quad \quad \quad \quad g_{2z1} \propto -\alpha_b + \mathcal{O}(\theta\alpha_b) \\
 \end{array}
 \quad
 \begin{array}{c}
 h_2 \text{---} \swarrow \quad \searrow \quad \text{Z} \\
 \quad \quad \quad h_1 \quad \quad \quad \quad \quad \quad g_{3z1} \propto -\theta + \mathcal{O}(\alpha_b^2)
 \end{array}$$



Now Let's move on to the results. First I will discuss about the results in the alignment limit, specifically in the Type-I model. The left plot is the current exclusion limit, and the right one is the future projected limit. The vertical axis is ... which denote the level of CP violation. the horizontal axis is the tanbeta. The pink region is excluded by the theoretical constraints: stability, unitarity and the existence of real solution for alphac in terms of alphab. The orange region is the current LHC limit from a search of the heavy higgs to Zh, and this blue and magenta region projected future LHC limit with 300 and 3000 inverse fb respectively. The light red is the mercury edm, the blue is the electron EDM, the green is the neutron EDM. Let me remind you that in the alignment limit the coupling between h3 and Zh is highly suppressed, so the LHC exclusion limit mainly comes from the exclusion of h2. One can find that in the low tanbeta region the electron EDM is very powerful, this is due to the fact that the pseudoscalar coupling between higgs and fermion will be enhanced by cotbeta. However the Collider search cannot fully take advantage of this enhancement because the increasing coupling to the b quark will reduce the branching ratio for h2 decay to Zh.

Results

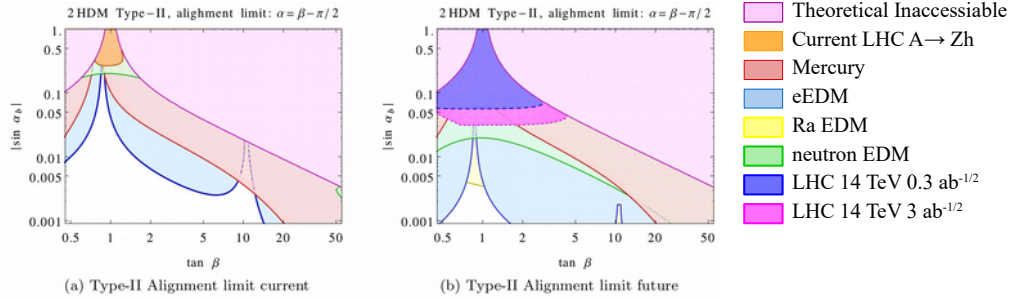
- Alignment limit
Type-I



One should also notice that there is a small piece in the future collider exclusion region is chopped by us. This is because, in this region the amplitude for the resonance production becomes comparable to that of non-resonant box diagram. So the shape of the signal distribution might not be approximated by our simple simulation. In that case we do not trust our analysis in that region.

Results

- Alignment limit
Type-II



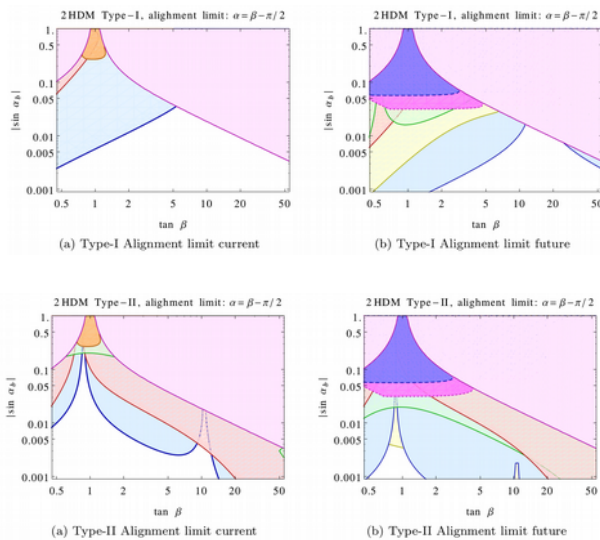
$$\begin{aligned}\tilde{c}_{1,b} &= -\alpha_b \tan \beta \\ \tilde{c}_{2,b} &= \alpha_c \tan \beta \\ \tilde{c}_{3,b} &= \tan \beta\end{aligned}$$

$$\begin{aligned}c_{1,b} &= 1 \\ c_{2,b} &= \tan \beta \\ c_{3,b} &= -\alpha_c \tan \beta - \alpha_b\end{aligned}$$

The situation is pretty similar in the type II model for the collider exclusion. However the shape of EDM exclusion is changed lot, the most prominent one is that the electron EDM will present the cancellation around $\tan\beta = 1$. And also one should notice that the neutron EDM does not have this limitation, and it will outperform the collider search.

Results

- Summary for the alignment limit



- LHC make a discovery:

Type-I will at least give non-zero
Ra , electron EDM
Otherwise, falsify Type-I.

Type-II will give non-zero
Neutron and Ra EDM
Otherwise, falsify Type-II.

- LHC gives null result:

Does not preclude the possibility for
small CP Violation in 2HDM

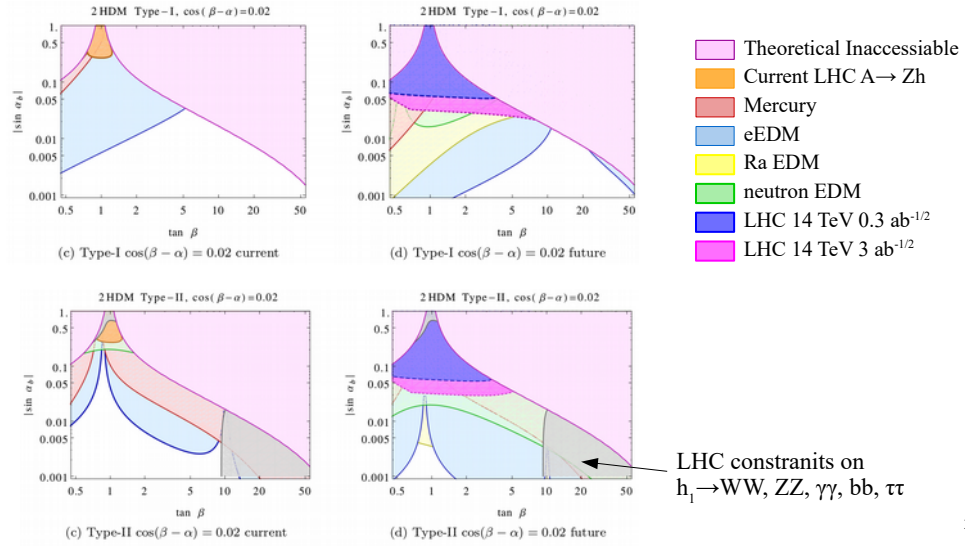
EDM result may or may not falsify
the CPV 2HDM

Here is the summary for the alignment limit. If our nature is realized by the 2HDM in the alignment limit, then If future LHC make a discovery, then one can immediately conclude that there is a CP violation in the 2HDM, and expected to see the corresponding EDM signal. In this case if EDM gives null results then CPV 2HDM is falsified.

If LHC gives null result then it does not preclude the possibility for small CP violation in 2HDM. Non zero EDM result may or may not falsify the CPV2HDM depending on the value of the EDM. For example if the EDM result corresponding the point in the region that sensitive by the LHC limit then CPV2DHM is falsified

Result

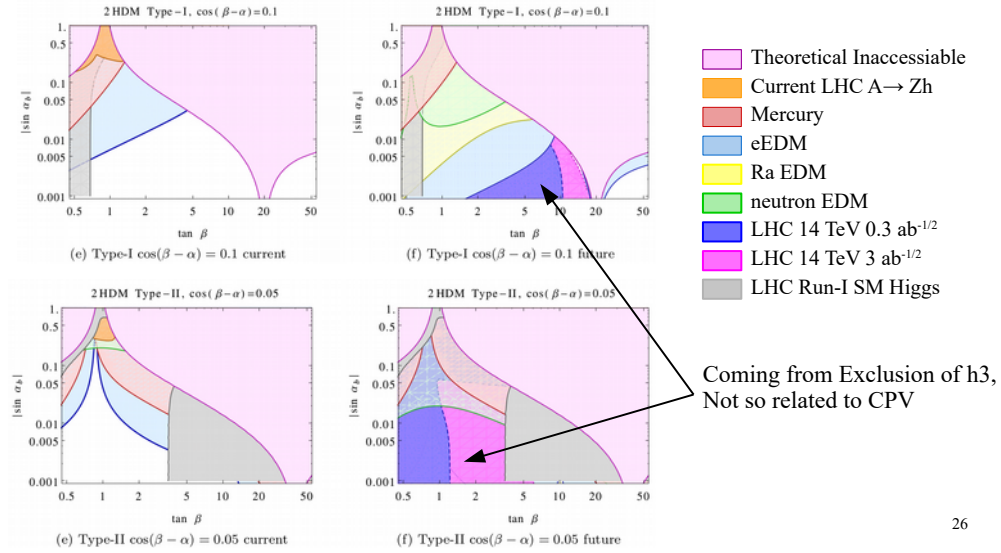
- Small deviation from the alignment limit



Result

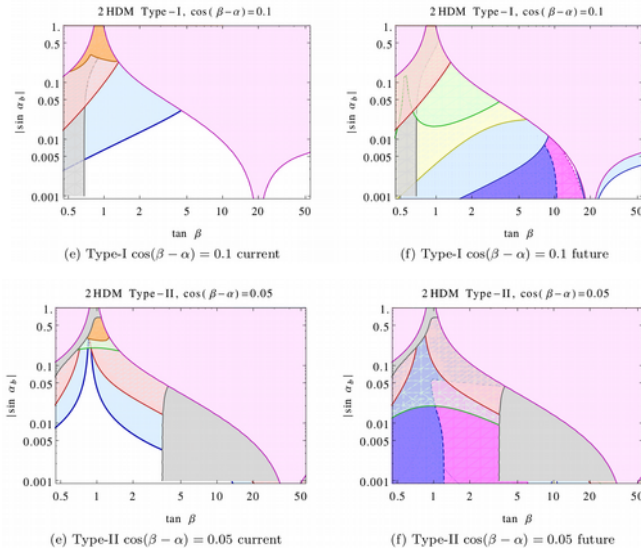
$$\begin{array}{c}
 h_2 \text{---} \swarrow \quad \searrow \\
 \quad \quad \quad Z \quad \quad h_1 \\
 \quad \quad \quad g_{2z1} \propto -\alpha_b + \mathcal{O}(\theta\alpha_b)
 \end{array}
 \quad
 \begin{array}{c}
 h_1 \text{---} \swarrow \quad \searrow \\
 \quad \quad \quad Z \quad \quad h_1 \\
 \quad \quad \quad g_{3z1} \propto -\theta + \mathcal{O}(\alpha_b^2)
 \end{array}$$

- Large deviation from the alignment limit



Result

- Large deviation from the alignment limit



- LHC make a discovery:

One may not conclude that there is a sizeable CPV effect. Need further CP information of the newly discovered particle.

- LHC gives null results:
A non-zero EDM result will falsify CPV 2HDM.

Summary

- Discussed the CPV condition in the 2HDM
- The $h_{23} \rightarrow Zh_1$ is a good process to constraint CP
- EDM experiments will generally better than collider experiments in testing CPV, while the interplay of both experiments will help to falsify CPV 2HDM.

Back up

- Detail of Basis Invariants

$$I_1 = I_3 = 0 \quad \text{due to } \lambda_6 = \lambda_7 = 0$$

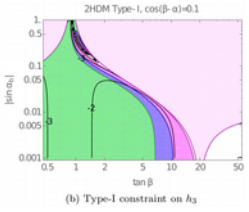
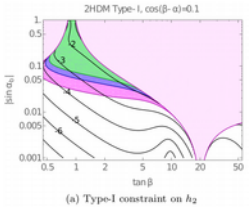
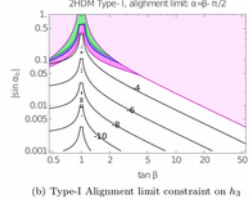
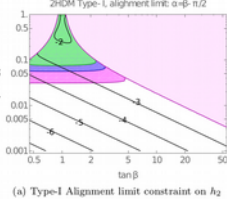
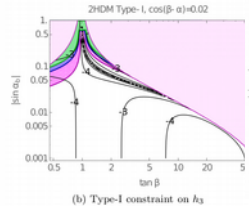
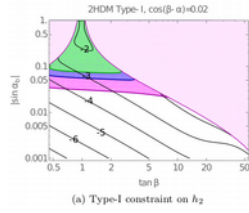
$$I_2 = (\lambda_1 - \lambda_2)[\text{Im}((m_{12}^2)^2 \lambda_5^*)]$$

$$I_4 = 1/2[(\lambda_1 - \lambda_3 - \lambda_4)(\lambda_2 - \lambda_3 - \lambda_4) - |\lambda_5^2|] \\ \times (m_{22}^2 - m_{11}^2) \text{Im}((m_{12}^2)^2 \lambda_5^*)$$

$$J_1 = (\lambda_1 - \lambda_2) \text{Im}(m_{12}^2)$$

$$J_2 = 1/2 v_1 v_2 (v_1 v_2 (m_{11}^4 - m_{22}^4) \text{Im}(\lambda_5) \\ + (m_{11}^2 v_1^2 (\lambda_3 + \lambda_4 - \lambda_1) + m_{22}^2 v_2^2 (\lambda_2 - \lambda_3 - \lambda_4)) \text{Im}(m_{12}^2))$$

Backup



Backup

$$\lambda_1 = \frac{m_{h_1}^2 \sin^2 \alpha \cos^2 \alpha_b + m_{h_2}^2 R_{21}^2 + m_{h_3}^2 R_{31}^2}{v^2 \cos \beta^2} - \nu \tan^2 \beta ,$$

$$\lambda_2 = \frac{m_{h_1}^2 \cos^2 \alpha \cos^2 \alpha_b + m_{h_2}^2 R_{22}^2 + m_{h_3}^2 R_{32}^2}{v^2 \sin \beta^2} - \nu \cot^2 \beta ,$$

$$\text{Re} \lambda_5 = \nu - \frac{m_{h_1}^2 \sin^2 \alpha_b + \cos^2 \alpha_b (m_{h_2}^2 \sin^2 \alpha_c + m_{h_3}^2 \cos^2 \alpha_c)}{v^2} ,$$

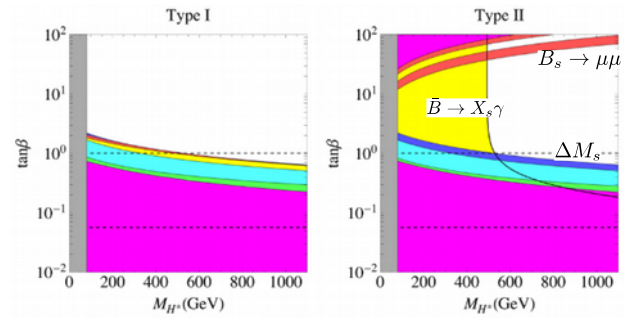
$$\lambda_3 = \nu - \frac{m_{h_1}^2 \sin \alpha \cos \alpha \cos^2 \alpha_b - m_{h_2}^2 R_{21} R_{22} - m_{h_3}^2 R_{31} R_{32}}{v^2 \sin \beta \cos \beta} - \lambda_4 - \text{Re} \lambda_5 ,$$

$$\text{Im} \lambda_5 = \frac{2 \cos \alpha_b [(m_{h_2}^2 - m_{h_3}^2) \cos \alpha \sin \alpha_c \cos \alpha_c + (m_{h_1}^2 - m_{h_2}^2 \sin^2 \alpha_c - m_{h_3}^2 \cos^2 \alpha_c)^2 \sin \alpha \sin \alpha_b]}{v^2 \sin \beta}$$

$$\tan \beta = \frac{(m_{h_2}^2 - m_{h_3}^2) \cos \alpha_c \sin \alpha_c + (m_{h_1}^2 - m_{h_2}^2 \sin^2 \alpha_c - m_{h_3}^2 \cos^2 \alpha_c) \tan \alpha \sin \alpha_b}{(m_{h_2}^2 - m_{h_3}^2) \tan \alpha \cos \alpha_c \sin \alpha_c - (m_{h_1}^2 - m_{h_2}^2 \sin^2 \alpha_c - m_{h_3}^2 \cos^2 \alpha_c) \sin \alpha_b} .$$

Back up

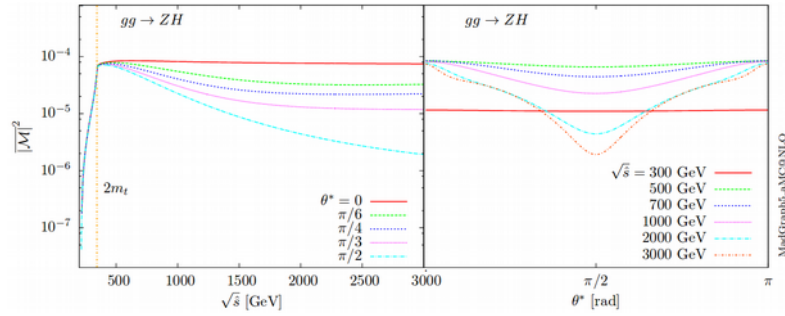
- Flavor Constraint



T. Enomoto and R. Watanabe, J. High Energy Phys. 05(2016) 002.

Backup

- Box interference

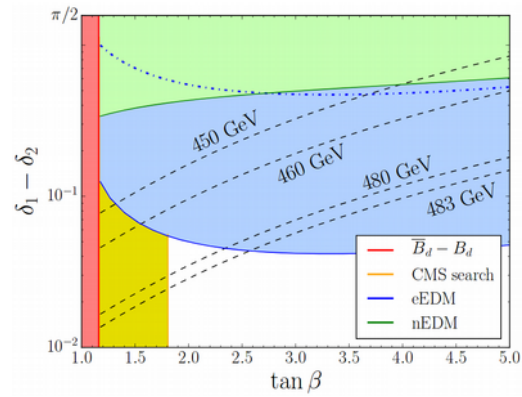


$$|\mathcal{M}|_{res,peak}^2 > 10^{-4}$$

B. Hespel, F. Maltoni, and E. Vryonidou, J. High Energy Phys. 06 (2015) 065

Backup

- Relation to Electroweak Bayrogenesis



G. C. Dorsch, S. J. Huber, T. Konstandin, and J. M. No, J. Cosmol. Astropart. Phys. 05 (2017) 052.